Zoological Journal of the Linnean Society, 2020, **190**, 974–1001. With 18 figures.

Hide-and-seek with hoverflies: *Merodon aureus* – a species, a complex or a subgroup?

ANTE VUJIĆ[1], LJILJANA ŠAŠIĆ ZORIĆ[2*], JELENA AČANSKI[2], LAURA LIKOV[1], SNEŽANA RADENKOVIĆ[1], MIHAJLA DJAN[1], DUBRAVKA MILIĆ[1], ANJA ŠEBIĆ[1], MILICA RANKOVIĆ[1] and SAMAD KHAGHANINIA[3]

[1]*University of Novi Sad, Faculty of Sciences, Trg Dositeja Obradovića 3, 21000 Novi Sad, Serbia*
[2]*University of Novi Sad, BioSense Institute, Dr Zorana Đinđića 1, 21000 Novi Sad, Serbia*
[3]*University of Tabriz, Faculty of Agriculture, Department of Plant Protection, Tabriz, Iran*

Received 14 July 2019; revised 28 December 2019; accepted for publication 14 February 2020

In order to disentangle the currently confused interpretations and nomenclature of *Merodon aureus* and *M. aeneus*, we have reviewed all existing type material and species names known to us as assigned synonyms of these taxa. We resolve *M. aeneus* as being a junior synonym of *M. aureus*. We designate a lectotype for *M. aureus* and a neotype for *M. aeneus*. Additionally, we provide evidence that *M. aureus*, together with two newly discovered taxa (***M. calidus* sp. nov.** and ***M. ortus* sp. nov.**), represent a complex of cryptic species named the *M. aureus* species complex. This complex, together with the *M. unicolor* species complex and the species *M. pumilus*, is part of the *M. aureus* subgroup. The *M. unicolor* species complex comprises two cryptic species: *M. unicolor* and ***M. albidus* sp. nov**. The new species are described by applying an integrative taxonomic approach using several data types (*COI* and 28S rRNA genes, geometric morphometry of the wings, ecological and distributional data). Based on the *COI* gene sequence analysis and distributional data, the pupa previously described as an immature stage of the species *M. aureus* is redefined as an immature stage of the new species *M. calidus*. Speciation within the *M. aureus* subgroup is discussed in the context of the phylogeographic history in the studied region.

ADDITIONAL KEYWORDS: cryptic taxa – distribution – DNA sequences – environmental niche modelling – geometric morphometry – identification key – new species – Palaearctic.

INTRODUCTION

Merodon Meigen, 1803 is one of the few phytophagous genera of hoverflies. It comprises more than 160 species distributed in Palaearctic and Afrotropical regions (Ståhls *et al.*, 2009). *Merodon* is the largest hoverfly genus in Europe, where 120 species are recognized (Vujić *et al.*, 2015). The considerable diversity of this genus, particularly in the Mediterranean region, is linked to the large diversity of geophytes in this region, on which *Merodon* larvae feed (Ricarte *et al.*, 2008; Andrić *et al.*, 2014). Adults of *Merodon* morphologically mimic bumblebees and bees (Hymenoptera: Apidae) and feed on pollen and nectar from early spring to late autumn (Speight, 2018). Recent taxonomic papers dealing with the genus *Merodon* have examined different groups of species and identified many taxa new to science (Marcos-García *et al.*, 2011; Radenković *et al.*, 2011, 2018a, b; Vujić *et al.*, 2012, 2015, 2018; Ačanski *et al.*, 2016; Šašić *et al.*, 2016; Šašić Zorić *et al.*, 2018).

The identity of the taxon described under the name *Merodon aureus* by Fabricius (1805) is still subject to debate. This name was re-established by the Biosystematic Database of World Diptera (Thompson & Brake, 2005), with *M. aeneus* Megerle in Meigen, 1822 being assigned as a synonym. For decades, authors used the name *M. aeneus* for a small species (8–12 mm) with a short, rounded abdomen and a distinct spine on the metatrochanter in males, distributed in central and south Europe (Šimić & Vujić, 1997; Schmid, 1999; Van de Weyer & Dils, 1999; Speight, 2018). Based on the original descriptions associated with both these species names, and after examining museum material from Germany

*Corresponding author. E-mail: ljsasic@biosense.rs
[Version of record, published online 4 April 2020; http://zoobank.org/ urn:lsid:zoobank.org:pub:F3A3CAA9-85B9-47F3-B657-06DA9A2897CB]

and Austria, Marcos-García *et al.* (2007) decided to adopt the synonymy established in Thompson & Brake (2005). They used the term '*aureus* group' and presented members of the group from the Iberian Peninsula: *M. chalybeus* Wiedemann in Meigen, 1822, *M. funestus* (Fabricius, 1794), *M. legionensis* Marcos-García *et al.*, 2007, *M. pumilus* Macquart in Lucas, 1849, *M. quercetorum* Marcos-García *et al.*, 2007 and *M. unguicornis* Strobl in Czerny & Strobl, 1909. In a publication on the integrative taxonomy of Iberian *Merodon* species, Mengual *et al.* (2006) identified a group of the same Iberian species (except *M. pumilus*) as being one of four main clades within the genus. Using cytochrome *c* oxidase subunit I (*COI*) gene sequence analysis, Radenković *et al.* (2018a) recognized four lineages within the genus *Merodon*: *albifrons+desuturinus*, *aureus* (*s.l.*), *avidus–nigritarsis* and *natans*.

Šašić *et al.* (2016) proposed a system of four levels for classifying the genus *Merodon* and defined large monophyletic clades [corresponding to the lineages in Radenković *et al.* (2018a)] as the first level of this classification. They resolved four main clades, each of which comprised multiple morphologically divergent species groups (*aureus*, *albifrons*, *desuturinus* and *avidus*). For instance, within the *aureus* clade, the authors introduced five morphologically defined species groups (*aureus*, *funestus*, *nanus*, *spinitarsis* and *bombiformis*), representing the second level of their proposed classification scheme. The third level consists of subgroups of species having similar morphologies, but exhibiting small, consistent, interspecific differences. The *M. aureus* species group consists of *aureus*, *dobrogensis*, *bessarabicus*, *cinereus* and *chalybeus* subgroups. These subgroups are themselves constituted of species complexes (the fourth classification level). These complexes include taxa that are morphologically inseparable based on classical taxonomic methods, but necessitate an integrative taxonomic approach, involving molecular markers, geometric morphometry and ecological data, to be distinguished. Apart from the species complexes within its subgroups, the *M. aureus* species group also contains the *M. caerulescens* species complex and the distinctive species *M. unguicornis* that cannot be assigned to any subgroups (Šašić *et al.*, 2016; Šašić Zorić *et al.*, 2018).

Previous research on the *M. aureus* species group discovered that the *M. aureus* and *M. cinereus* species complexes each comprise three species: *M. aureus* A, B, C and *M. cinereus* A, B, C (Milankov *et al.*, 2008). *Merodon cinereus* B was later described as an independent complex of three cryptic species and was named the *M. atratus* species complex (*cinereus* subgroup) (Šašić *et al.*, 2016). Radenković *et al.* (2018b) resolved the *M. luteomaculatus* species complex (six cryptic species), which had initially been introduced in a detailed revision of the *M. bessarabicus* subgroup (Veselić *et al.*, 2017), while Šašić Zorić *et al.* (2018) described new species within the *M. caerulescens* species complex. The cryptic species in all of these complexes have been resolved using integrative taxonomy based on morphology, molecular analyses, geometric morphometry, environmental niche comparisons and/or distributional data (Fig. 1).

In this study, we continue our characterization of the *M. aureus* species group, focussing on the *M. aureus* subgroup. Our aims are to: (1) review the identity and nomenclature of *M. aureus* and *M. aeneus*, (2) define and describe taxa within the *M. aureus* subgroup, (3) delimit species within the subgroup using integrative taxonomy and (4) evaluate the potential of molecular data (mtDNA *COI* gene, 28S rRNA gene), geometric morphometrics and environmental niche modelling to support species delimitations.

MATERIAL AND METHODS

Material

The specimens were collected with a hand net. In total, 1330 *Merodon* specimens belonging to the *M. aureus* subgroup were collected in Morocco, Algeria, Tunisia, Portugal, Spain, Andorra, France, Switzerland, Germany, Italy, Austria, Slovenia, Croatia, Bosnia and Herzegovina, Serbia, Montenegro, Albania, North Macedonia, Bulgaria, Romania, Greece, Turkey, Iran and Azerbaijan. Specimen sampling was performed over the course of a 181-year-period (for details, see 'Type material' and Supporting Information, Appendix S1). Most of the material used for molecular analyses was collected by the authors (from Switzerland: Swiss Alps; Italy: Apuane mountains and Italian Alps; Morocco: Beni-Snassen Mountains; Spain: Sierra Nevada mountain range; Bosnia and Herzegovina: Romanija; Montenegro: Durmitor, Orjen, Prokletije and Rumija; Serbia: Stara Planina, Kopaonik, Zlatar and Đerdap; Greece: Peloponnese). Geographic distributions were processed in DivaGis (v.7.5).

Depositories

The type materials of all described European species within the *M. aureus* subgroup *sensu* Šašić *et al.* (2016) were studied. Considerable effort was made to locate true type specimens of *M. aureus* and *M. aeneus*, which have long been considered lost. In addition, specimens of the *M. aureus* subgroup deposited in the museums and universities listed below, including both published and unpublished records, were studied and analysed: A. S. coll., Axel Ssymank collection, Germany; BMNH, Natural History Museum, London, UK; CNHM,

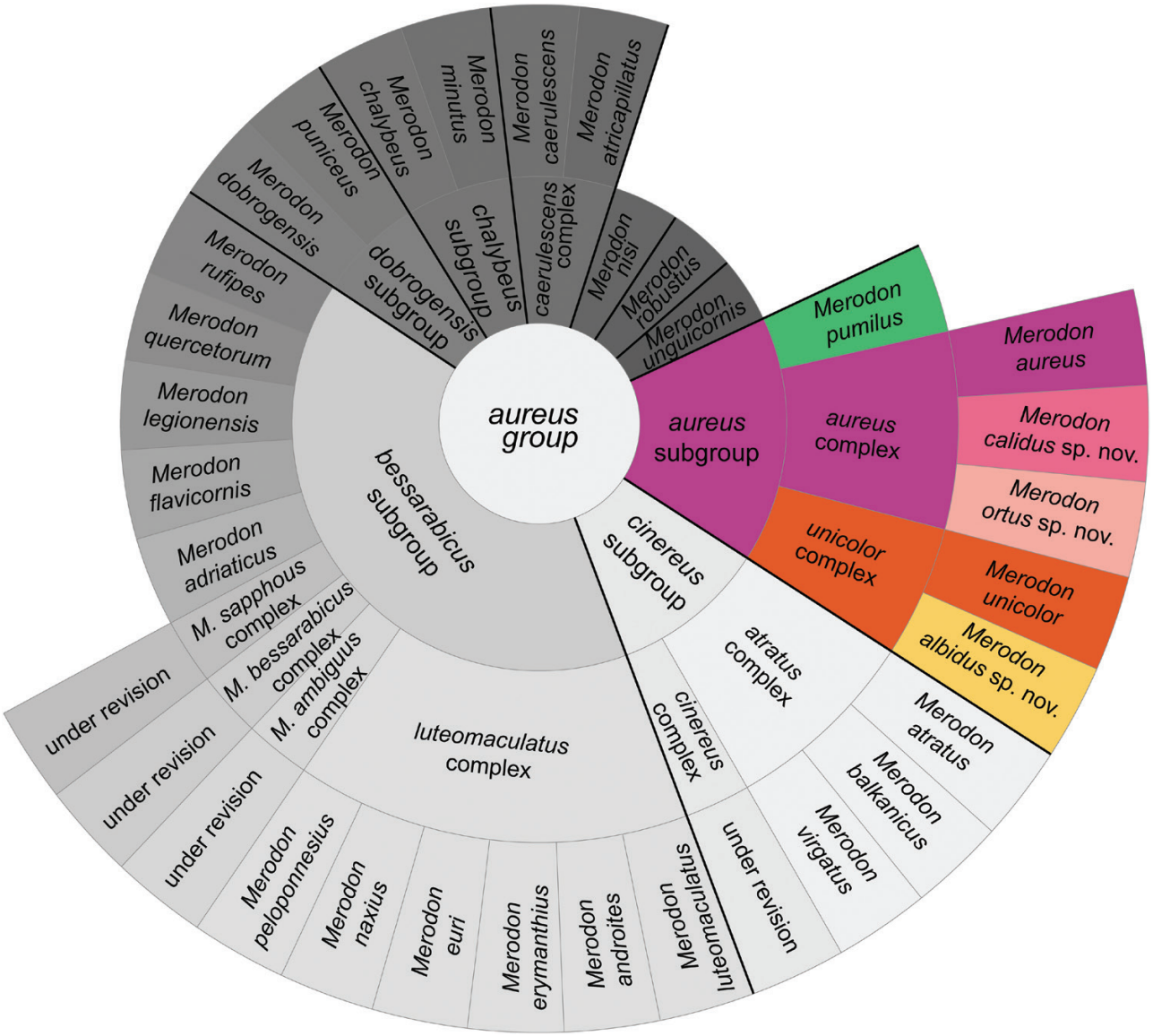

Figure 1. The known diversity of the *Merodon aureus* species group. Hierarchical levels of classification are illustrated as concentric circles in an outward declining trend.

Croatian Natural History Museum, Zagreb, Croatia; D. D. coll, Dieter Doczkal collection, Germany; FSUNS, Faculty of Sciences, Department of Biology and Ecology, University of Novi Sad, Novi Sad, Serbia; H. M. M. coll., Hasan Maleki Milani collection, Iran; HMIM, Hayk Mirzayans Insect Museum, Insect Taxonomy Research Department, Iranian Research Institute of Plant Protection, Tehran, Iran; J. D. coll., Jos Dils collection, Belgium; J. H. coll., Jiří Halada collection, Czech Republic; J. S. coll, John T. Smit collection, the Netherlands; J. v. S. coll., Jeroen van Steenis collection, the Netherlands; M. B. coll., Miroslav Bartak collection, Czech Republic; M. C. coll., Michael de Courcy Williams collection; M. H. coll., Martin Hauser collection, USA; M. J. S. coll., M. J. Smart collection, UK; MNCN, Museo Nacional de Ciencias Naturales, Madrid, Spain; MNHN, Musee National d'Histoire Naturelle, Paris, France; MZH, Finnish Museum of Natural History, University of Helsinki, Helsinki, Finland; NHMW, Naturhistorisches Museum Wien, Vienna, Austria; NMNHS, National Museum of Natural History, Sofia, Bulgaria; PMCG; Prirodnjački muzej, Podgorica, Crna Gora (Natural history museum); R. H. coll., Rüstem Hayat collection, Turkey; NBCN (former RMNH), Naturalis Biodiversity Center, Leiden, Netherlands; S. P. coll., Stefan Pruner collection, Austria; SMNS, Staatlichen Museum für Naturkunde Stuttgart, Germany; W. v. S. coll, Wouter van Steenis collection, Netherlands; WML, World

Museum Liverpool, Liverpool, UK; ZHMB, Zoologisches Museum of the Humboldt University, Berlin, Germany; ZMBH, National Museum of Bosnia and Herzegovina, Sarajevo, Bosnia and Herzegovina; ZMUC, Zoological Museum, Natural History Museum of Denmark, University of Copenhagen, Copenhagen, Denmark. Every specimen is assigned a number next to the collection abbreviation and this is a unique identifier in the list of specimens.

Morphological and taxonomic studies

Dry, male specimens were relaxed in a humidity chamber, and genitalia were extracted with an entomological pin. Genitalia were cleared by boiling in 10% KOH solution for a few minutes. After clearing, genitalia were immersed in acetic acid and finally in ethanol to remove the acid before examination. Genitalia were stored in microvials containing glycerol and placed on the same pin as the specimen. Drawings were made with an FSA 25 PE drawing tube and digital photographs were taken with a Leica DFC 320 digital camera, both of which were attached to a binocular Leica MZ16 microscope. Measurements were taken using a micrometer. Morphological terms follow Thompson (1999), whereas those relating to male genitalia follow Marcos-García *et al.* (2007).

Molecular study

The genomic DNA of 158 hoverfly specimens (Supporting Information, Table S1) was extracted using the SDS (sodium dodecyl sulfate) extraction protocol described by Chen *et al.* (2010).

Polymerase chain reactions (PCR) were carried out in 25-μL reaction volumes. The reaction mixture contained 1× reaction buffer (Thermo Scientific, Vilnius, Lithuania), 2.5 mM $MgCl_2$, 0.1 mM of each nucleotide, 1.25U Taq polymerase (Thermo Scientific, Vilnius, Lithuania), 5 pmol of each primer and approximately 50 ng of template DNA. PCR amplifications were performed using the following conditions: 95 °C for 2 min; 29 cycles of 94 °C for 30 s each, 49 °C (for the 3' end of the *COI* gene) or 50 °C (for the 5' end of the *COI* gene and D2-3 region of the 28S rRNA gene) for 30 s; 72 °C for 2 min; with a final extension at 72 °C for 8 min. Amplification of the aforementioned gene regions was carried out using an Eppendorf Personal Thermocycler and Applied Biosystems Veriti 96 Well Thermal Cycler. The commercial primers C1-J-2183 (also known as Jerry) and TL2-N-3014 (also known as Pat) were used for amplification and sequencing of the *COI* 3' end (Simon *et al.*, 1994), LCO1490 and HCO2198 (Folmer *et al.*, 1994) were used for the *COI* 5' end (barcode sequence) and F2 and 3DR (Belshaw *et al.* 2001) were employed for the D2-3 region of the 28S rRNA gene. PCR products were purified using Exonuclease I and FastAP Thermosensitive Alkaline Phosphatase (Thermo Scientific, Vilnius, Lithuania) according to the manufacturer's instructions. The PCR fragments were commercially sequenced in the forward direction by the Sequencing Laboratory of the Finnish Institute for Molecular Medicine (Helsinki, Finland) and Macrogen Europe (Amsterdam, Netherlands).

COI and 28S rRNA gene sequence analyses

The *COI* and 28S rRNA gene sequences were edited for base-calling errors using BioEdit 7.0.9.0. (Hall, 1999). The *COI* gene sequences were aligned manually, while 28S rRNA gene sequences were aligned using MAFFT v.7 (Katoh & Standley, 2013) and by applying Q-INS-i strategy in which secondary structure information of RNA is considered (Supporting Information, File S1). The 3' and 5' *COI* gene sequences were concatenated and combined into a single sequence matrix (Supporting Information, File S2). We downloaded from GenBank 5' *COI* gene sequences from the pupa and adults of the *M. aureus* species complex collected in Đerdap, Serbia (Preradović *et al.*, 2018). The 3' *COI* and 28S rRNA gene sequences were produced in this study. GenBank accession numbers of all sequences are provided in Supporting Information, Table S1. Maximum parsimony (MP) and maximum likelihood (ML) trees were constructed using the concatenated *COI* sequence matrix. Parsimony analysis was performed in NONA (Goloboff, 1999) spawned with the aid of Winclada ASADO (Nixon, 2008) using the heuristic search algorithm with 1000 random addition replicates (mult*1000), holding 100 trees per round (hold/100), maxtrees set to 100 000 and applying tree-bisection-reconnection (TBR) branch swapping. The bootstrap support values for clades were calculated with 1000 replicates. The ML tree was constructed using RAxML 8.2.8 (Stamatakis, 2014) using the CIPRES Science Gateway web portal (Miller *et al.*, 2010) under the general time-reversible (GTR) evolutionary model with a gamma distribution (GTRGAMMA) (Rodríguez *et al.*, 1990). Nodal supports were estimated using rapid bootstrapping with 1000 replicates. The trees were rooted with *Platynochaetus macquarti* Loew, 1862. We also included the following outgroups: *Eumerus amoenus* Loew, 1848, *E. pulchellus* Loew, 1848, *E. pusillus* Loew, 1848, *Merodon desuturinus* Vujić, Šimić & Radenković, 1995, *M. equestris* (Fabricius, 1794), *M. luteofasciatus* Vujić *et al.* in Vujić *et al.*, 2018 and *M. ruficornis* Meigen, 1822 (for GenBank accession numbers of all outgroups see Supporting Information, Table S1). The average uncorrected p distance matrix for concatenated *COI* gene sequences among species

belonging to the *M. aureus* subgroup was estimated using MEGA 7 software (Kumar *et al.*, 2016) with pairwise deletion of missing data. Since 28S rRNA gene sequences generally exhibit low overall variability among closely related species, we employed a Median-joining network of 28S rRNA genotypes [using the software NETWORK 5 (Bandelt *et al.*, 1999)], instead of MP or ML trees, to depict pairwise relationships among species within the *M. aureus* subgroup.

Geometric morphometric analysis

Geometric morphometric analysis of wing shape was conducted on 224 specimens of the *M. aureus* subgroup (Supporting Information, Table S1). Three separate geometric morphometric analyses were conducted: two for species identification within complexes of the *M. aureus* subgroup (*M. aureus* and *M. unicolor* complexes) and a third to explore phenotypic differentiation among geographically defined groups of specimens (herein treated as populations). Analyses within the *M. aureus* species complex were performed separately on males and females. Only three female specimens of the new taxon described below as *M. ortus* were available to us, so they were not included in our geometric morphometric analysis. The analysis of the *M. unicolor* species complex was conducted on a dataset in which both sexes were pooled and on the male dataset separately due to uneven sex distribution of available specimens. The right wing of each specimen was removed with microscissors and mounted in Hoyer's medium on a microscopic slide. Photo of the wing of the *M. aureus* lectotype specimen was taken by Mikkel Høegh Post from the Natural History Museum of Denmark. Wings have been archived and labelled with a unique code in the FSUNS collection, together with other data relevant to the specimens. High-resolution photographs of the wings were made using a Leica DFC320 video camera attached to a Leica MZ16 stereomicroscope. Eleven homologous landmarks at vein intersections or terminations were selected using TpsDig v.2.05 (Rohlf, 2006). Each wing was digitized three times to estimate the measurement error, and average landmark coordinates for each individual were used in analyses (Arnqvist & Mårtensson, 1998). Measurement error was found to be negligible.

Generalized least squares Procrustes superimposition was performed in MorphoJ v.2.0 (Klingenberg, 2011) on the raw landmark coordinates to minimize non-shape variations in location, scale and orientation of wings, and to superimpose the wings in a common coordinate system (Rohlf & Slice, 1990; Zelditch *et al.*, 2004). We conducted principal component analysis (PCA) on the Procrustes shape variables to reduce the dimensionality of our dataset. All further statistical analyses were conducted in the reduced space using a subset of independent principal components (PCs) that describe the highest overall classification percentage, calculated in a stepwise discriminant analysis (Baylac & Frieß, 2005).

To explore wing-shape variation among taxa, we employed canonical variate (CVA) and stepwise discriminant analysis (DA). Additionally, we used a Gaussian naïve Bayes' classifier to delimit species boundaries based on wing-shape variation without a prirori defined groups. Phenetic relationships among populations were determined by NJ analysis based on squared Mahalanobis distances computed from the discriminant function analysis applied to wing shape variables. A geophenogram was created using GenGIS v.2.4.1 (Parks *et al.*, 2013). Superimposed outline drawings produced in MorphoJ v.2.0 (Klingenberg, 2011) were used to visualize differences in mean wing shape among species pairs. All statistical analyses were performed in Statistica for Windows (Statistica, 2015).

Environmental niche modelling and niche differences

Environmental niche models (ENM) for each taxon were constructed using MaxEnt software (Phillips *et al.*, 2008) for the present time. To account for potential sampling bias in the investigated area, we generated a bias surface using SDMToolbox (Brown, 2014). More specifically, a Gaussian kernel density of sampling localities tool was loaded with presence points from species and we chose a sampling bias distance of 50 km. The obtained spatially filtered presence data and bias file were utilized in MaxEnt. Nineteen bioclimatic variables for current conditions were obtained from the WorldClim database (www.worldclim.org) at a 2.5-arc min resolution (Hijmans *et al.*, 2005). Covariates were first tested for multicollinearity for all species through VIF (various inflation factors) analysis in the R platform (R Development Core Team, 2016) using the package usdm (Naimi, 2015). To reduce the high level of collinearity, we sequentially dropped covariates with the highest VIF, then recalculated the VIFs and repeated this process until all VIFs were smaller than 10 (Montgomery & Peck, 1992). After this process, the remaining bioclimatic variables used for modelling the current potential distribution of our target hoverfly species were BIO2-Mean Diurnal Range, BIO4-Temperature Seasonality, BIO6-Min Temperature of Coldest Month, BIO8-Mean Temperature of Wettest Quarter, BIO9-Mean Temperature of Driest Quarter, BIO11-Mean Temperature of Coldest Quarter, BIO13-Precipitation of Wettest Month, BIO15-Precipitation

Seasonality, and BIO18-Precipitation of Warmest Quarter. We used the default parameters of MaxEnt and included 75% of species records for training and 25% for testing the model.

Final models from MaxEnt were used to measure niche overlap and to conduct similarity tests using ENM Tools (Warren *et al.*, 2008, 2010). Niche overlap between pairs of *Merodon* species was computed by means of Schoener's D (Schoener, 1968) for each comparison among pairs of models, ranging from 0 (no overlap) to 1 (complete overlap).

Similarity tests were used to evaluate if the examined species are more (= conserved) or less (= divergent) similar than expected based on the environmental differences in their ranges. If the true measured overlap values are significantly higher (or lower) than the values generated by the similarity test, the null hypothesis is rejected. This test was conducted in both directions since different directions may yield different results. Significance was tested using Statistica for Windows (Statistica, 2015).

RESULTS

Molecular analyses

We performed *COI* gene analyses on 176 concatenated 3' and 5' *COI* gene sequences (including outgroups). The total length of the *COI* alignment was 1400 bp. The total number of polymorphic sites within the ingroup sequence matrix was 194, of which 156 were parsimony informative.

MP analysis resulted in 13 equally parsimonious trees of 819 step lengths [consistency index (CI) = 59, retention index (RI) = 89], which we used to produce a strict consensus tree of 826 step lengths (CI = 59, RI = 89) (Supporting Information, Fig. S1). We also constructed a ML tree (Fig. 2). Both methods resulted in almost identical tree topologies when comparing strict consensus MP tree and ML tree, but with slight differences in bootstrap values for some of the clades (Fig. 2; Supporting Information, Fig. S1). The tree topologies resolved the following relations among species of the *M. aureus* subgroup: *M. pumilus*+ (*M. ortus* + (M. *unicolor*+ (*M. aureus*+ (*M. albidus* + *M. calidus*)))). The specimen AU713 from Greece that, according to its morphology, belongs to the *M. aureus* species complex, is linked to the *M. albidus* clade (of the *M. unicolor* species complex). Specimens of *M. calidus* from Stara Planina Mountain, Serbia (AU695–697, AU699 and AU169) and Kamena gora, Prijepolje, Serbia (AU1523) are misplaced and cluster with *M. aureus* specimens in a single clade. We found that pupa (L4) and adults collected from Đerdap, Serbia (AU363–367, AU701–AU705), reported by Preradović *et al.* (2018), lay within the *M. calidus* clade. All clades are supported with high bootstrap support, except *M. aureus* (ML – 68) and *M. calidus* (MP – 61, ML – 62).

Average uncorrected pairwise distances (p) between species pairs ranged from 0.8% (between *M. albidus* and *M. calidus*) to 8.4% (between *M. pumilus* and *M. ortus*) (Table 1).

Our 28S rRNA gene analysis included 154 sequences, which varied in length from 584 to 588 bp. Our alignment length was 588 bp, which included 12 variable positions, of which eight were parsimony informative. We identified a total of ten genotypes. Each of the species from the *M. aureus* species complex possessed unique 28S rRNA genotypes, whereas both species from the *M. unicolor* species complex shared one 28S rRNA genotype (Fig. 3; Supporting Information, Table S2).

Geometric morphometric data

Merodon aureus *complex*

We assessed wing-shape differences among males and females of *M. aureus* and the new species *M. calidus* and *M. ortus*. Stepwise discriminant analysis showed that all pairs of species differed significantly in wing shape (Table 2). Additionally, our DA correctly classified species, with an overall classification success of 96% for males and 98% for females. Among the 136 male specimens, six were misclassified: two *M. aureus* as *M. calidus*; three *M. calidus* specimens (as *M. aureus*) and only one specimen of *M. ortus* (as *M. calidus*). Among our female specimens, only one of 66 was misclassified (*M. aureus* as *M. calidus*). A similar outcome was obtained using the Gaussian naïve Bayes' classifier (94% of male and 98% of female specimens were correctly classified). Importantly, in both classifications, the *M. aureus* lectotype was correctly classified with posterior probability of 99%. Among male specimens, successive CVA generated two highly significant axes (CV1: Wilks' Lambda = 0.147; $\chi 2 = 241.446$; $P < 0.01$; CV2: Wilks' Lambda = 0.667; $\chi 2 = 50.9595$; $P < 0.01$). CV1 represents most of the wing-shape variation (88%) and describes wing-shape differences among *M. calidus* and the other two species, whereas CV2 (with 12% variation) separates males of *M. ortus* from the other two species (Fig. 4A). The most obvious wing-shape differences were among *M. calidus* and the other two species, whereas *M. aureus* and *M. ortus* exhibited the most similar wings (Fig. 4B). Females of *M. aureus* and *M. calidus* were separated along one highly significant CV axis (CV1: Wilks' Lambda = 0.2196; $\chi 2 = 83.3834$; $P < 0.01$).

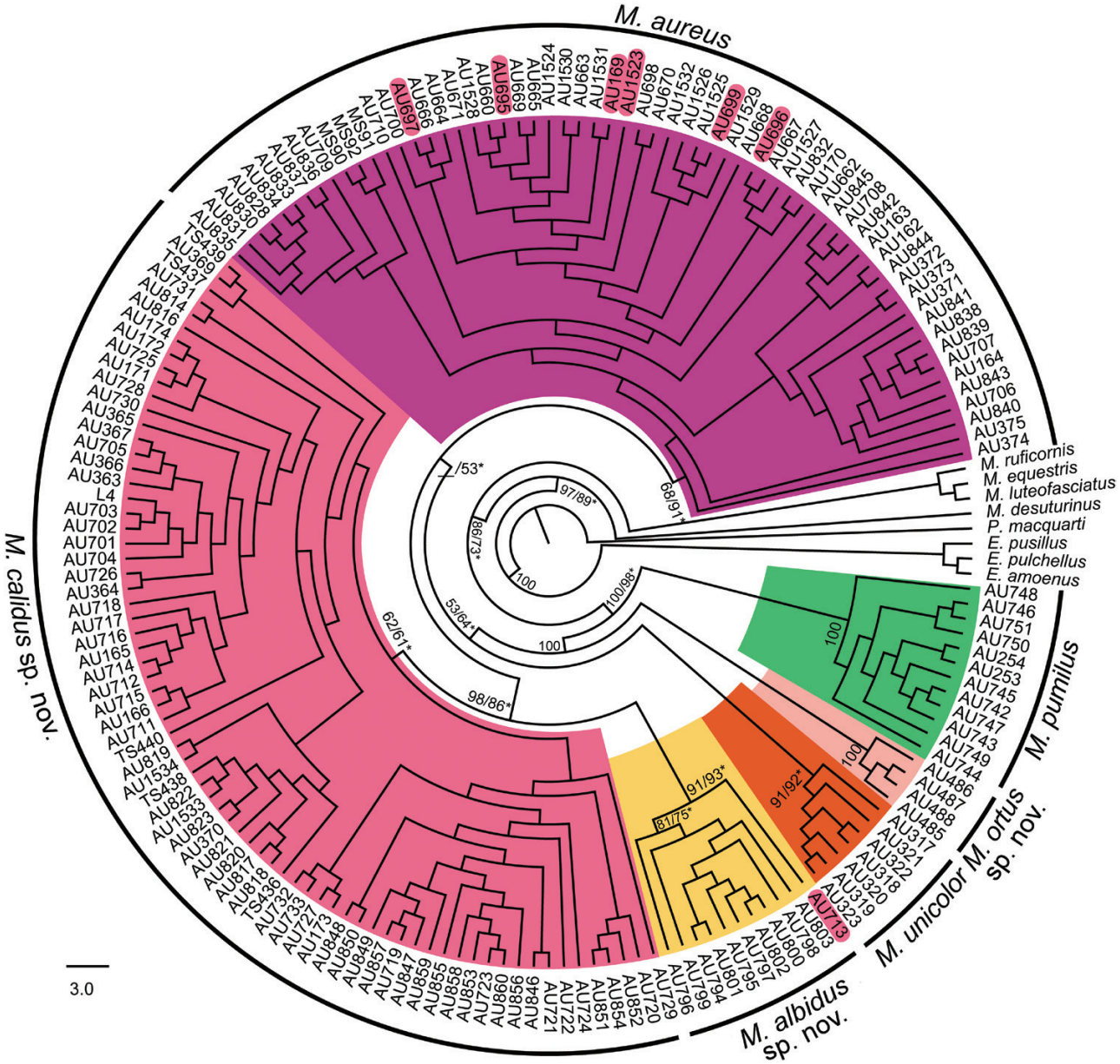

Figure 2. ML *COI* gene tree for species of the *Merodon aureus* subgroup. Specimen IDs in pink correspond to misplaced *M. calidus* specimens. Bootstrap support values for the main clades are indicated near nodes. Symbol: * indicate bootstrap values that differ in the MP tree from the respective value in the ML tree.

Table 1. Average uncorrected pairwise distances (p) between species pairs within *Merodon aureus* subgroup

Complex	Species	1.	2.	3.	4.	5.
***M. aureus* complex**	**1. *M. aureus***					
	2. *M. calidus*	0.010				
	3. *M. ortus*	0.021	0.023			
***M. unicolor* complex**	**4. *M. unicolor***	0.010	0.014	0.021		
	5. *M. albidus*	0.011	0.008	0.025	0.014	
	6. *M. pumilus*	0.080	0.081	0.084	0.080	0.081

Merodon unicolor *complex*

Geometric morphometric analyses of wing shape revealed the same pattern for pooled sexes and for the males separately, so we only present results based on the pooled dataset. Stepwise DA revealed that *M. unicolor* and *M. albidus* differed significantly in wing shape ($F_{10,21} = 76.5617, P < 0.01$), with an overall classification success of 100%. Moreover, the classification success of our Gaussian naïve Bayes' classifier was 97%. Only one specimen of *M. albidus* was misclassified as *M. unicolor*. The CVA generated one highly significant axis that differentiates *M. unicolor* from *M. albidus* (CV1: Wilks' Lambda = 0.0255; $\chi 2 = 88.0977$; $P < 0.01$). Differences in mean wing shape between these two species are depicted by superimposed outline drawings in Figure 4C.

Population-level analysis

We summarized the wing-shape relationships of all analysed populations using an NJ phenogram based on squared Mahalanobis distances computed from the DA. The resulting phenogram showed that all conspecific populations cluster according to species and that two sympatric populations of *M. aureus* and *M. calidus* from Stara Planina (Serbia) have clearly distinct wing shapes (Fig. 5).

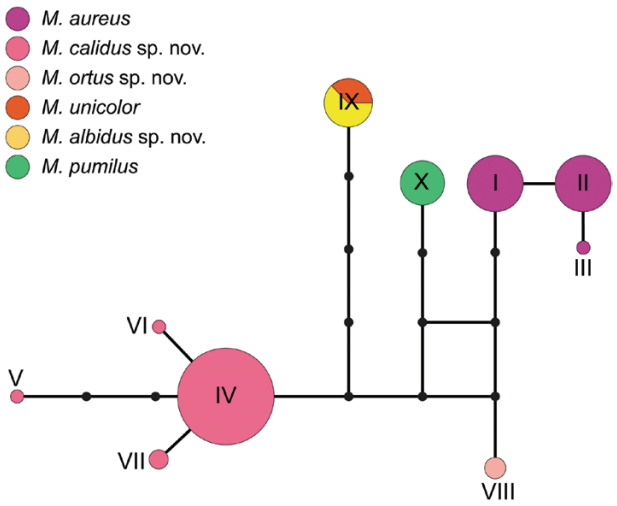

Figure 3. Genotype network (28S rRNA gene) of the *Merodon aureus* subgroup.

ENVIRONMENTAL NICHE COMPARISONS FOR THE *MERODON AUREUS* SUBGROUP

Niche overlap among investigated *Merodon* species was generally low (Table 3). The greatest degree of niche overlap was exhibited by the *M. aureus–M. calidus* and M. *pumilus–M. unicolor* species pairs (0.30 and 0.21, respectively), but is still considered low. Other investigated species pairs show no spatial overlap in their ENMs (Table 3).

The results of our similarity tests suggest that niche divergence is by far the most common pattern observed in these hoverflies when assessed using overall niche model characteristics (Table 3). A single exception was observed for the *M. aureus–M. calidus* pair, which showed significant niche conservation.

TAXONOMY

Using a classical morphological approach, we were able to identify three species (*M. aureus*, *M. unicolor* and *M. pumilus*) within the *M. aureus* subgroup, but molecular and geometric morphometric analyses revealed additional morphologically cryptic species (Fig. 6). These new cryptic species are closely related to morphologically described species, forming complexes that we name the *M. aureus* species complex and the *M. unicolor* species complex.

The *M. aureus* species complex contains three species: one previously recognized and two here described. These are the nominal species *M. aureus* distributed in the high mountains of central Europe (Fig. 7), the new species *M. calidus* recorded from the Mediterranean and sub-Mediterranean mountains

Table 2. Results of discriminant analysis conducted on wing shape variables. F values are shown above the diagonal, *P* values are shown below the diagonal, separately for males and females

	M. aureus	***M. calidus***	***M. ortus***
	Males (d.f. = 15, 120)		
M. aureus		28.01063	5.106169
M. calidus	$P < 0.001$		5.206877
M. ortus	$P < 0.001$	$P < 0.001$	
	Females (d.f. = 18, 47)		
M. aureus		9.280545	
M. calidus	$P < 0.001$		

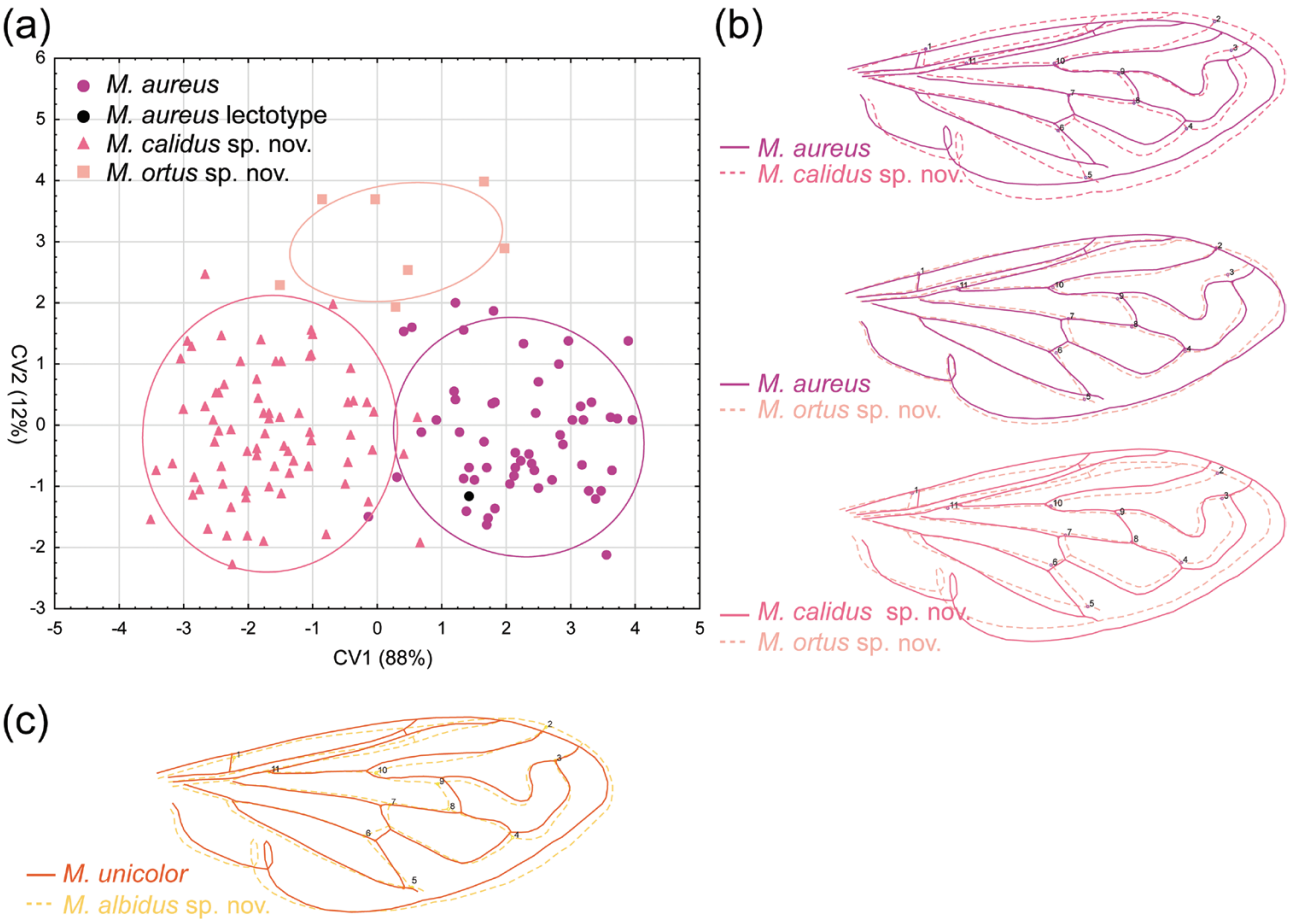

Figure 4. Geometric morphometric analyses of wing shape among species of the *Merodon aureus* subgroup. A, scatter plot of individual scores of CV1 and CV2 among males of *M. aureus*, *M. calidus* and *M. ortus*. Superimposed outline drawings showing differences in average wing shape for each species pair. B, males of *M. aureus*, *M. calidus* and *M. ortus*. C, species from the *M. unicolor* species complex. Differences in the average wing shapes among species pairs have been exaggerated three-fold to make them more visible.

of the Balkan Peninsula (Fig. 7) and the new species *M. ortus* distributed in the high mountains around the southern Caspian Sea (Fig. 7).

The *M. unicolor* species complex includes two species: the nominal species *M. unicolor* distributed in the Pyrenees and the Iberian Peninsula (Fig. 8) and the new species *M. albidus* discovered in the Anatolian Peninsula (Fig. 8).

Merodon pumilus is a species distinct from the two previously mentioned complexes and is distributed in the Iberian Peninsula and Morocco (Fig. 9).

MERODON AUREUS GROUP *SENSU* RADENKOVIĆ *ET AL.* (2011)

Diagnosis: Mesocoxa posteriorly with long pile. Anterior anepisternum with a pilose area ventral to postpronotum. In male genitalia, anterior surstyle lobe undeveloped (Fig. 10A). Small-sized (8–13 mm) species with a short, rounded abdomen, a distinct spine on the metatrochanter in males (Fig. 11B marked with white arrow) and a characteristic structure of the male genitalia: posterior surstyle lobe with parallel margins and rounded apex (Fig. 10A) and a narrow, elongated, sickle-shaped hypandrium without lateral sclerite of aedeagus (Fig. 10B, C).

MERODON AUREUS SUBGROUP *SENSU* ŠAŠIĆ *ET AL.* (2016)

Diagnosis: Species with golden reflection and rough punctate scutum and terga (Fig. 11). Mesonotum (in both sexes) and terga (in male) covered with only pale pile, reddish to yellow-grey. Tibiae and tarsi predominantly black (Fig. 11B). Terga uniformly dark.

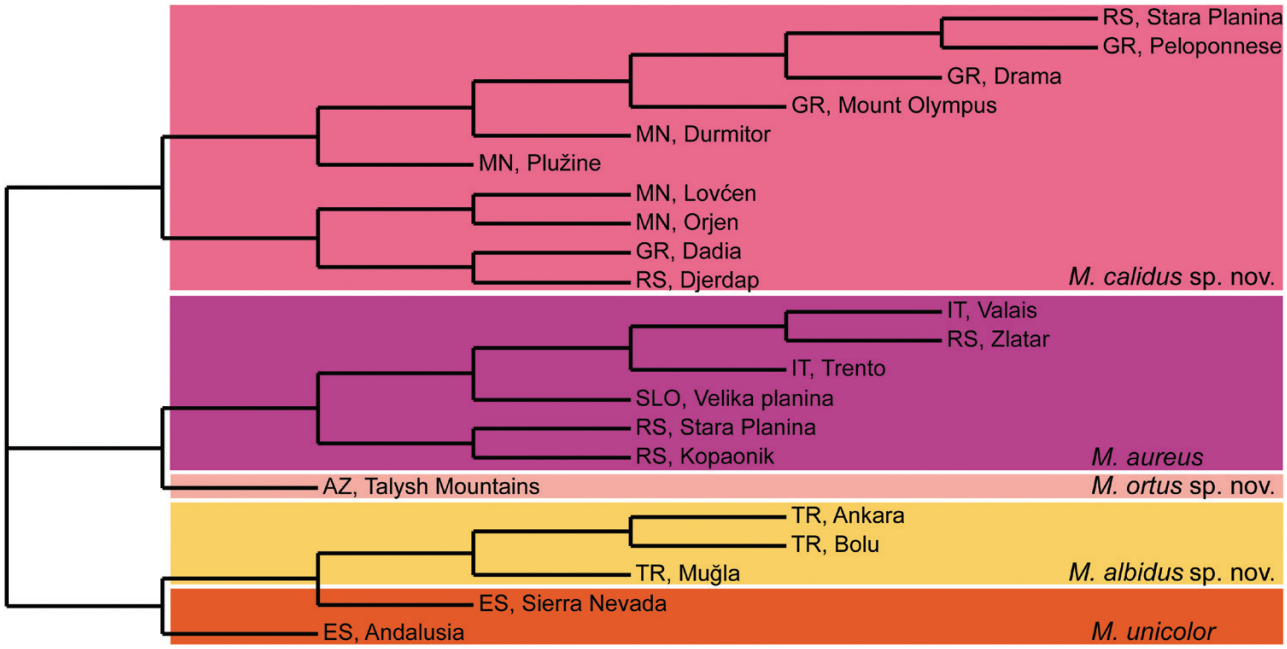

Figure 5. NJ phenogram constructed using squared Mahalanobis distances of wing shape for populations of species of the *Merodon aureus* subgroup.

Table 3. Tests of niche overlap (Schoener's D) and niche similarity for species of *Merodon aureus* subgroup

***Merodon* species**		**Niche overlap**	**Niche similarity test (± SD)**	
A	**B**		**A vs. B**	**B vs. A**
M. albidus	***M. aureus***	0.00072	0.00215 ± 0.00072**	0.00455 ± 0.00148**
M. albidus	***M. calidus***	0.00129	0.00699 ± 0.00396**	0.00432 ± 0.00142**
M. albidus	***M. ortus***	0.00080	0.00076 ± 0.00047NS	0.00601 ± 0.00111**
M. albidus	***M. pumilus***	0.00139	0.00180 ± 0.00036**	0.00196 ± 0.00082**
M. albidus	***M. unicolor***	0.00137	0.00067 ± 0.00028**	0.00257 ± 0.00088**
M. aureus	***M. calidus***	0.30545	0.26057 ± 0.03193**	0.22887 ± 0.01947**
M. aureus	***M. ortus***	0.00146	0.00338 ± 0.00153**	0.00489 ± 0.00153**
M. aureus	***M. pumilus***	0.00087	0.10982 ± 0.04063**	0.00306 ± 0.00102**
M. aureus	***M. unicolor***	0.01924	0.00184 ± 0.00064**	0.00192 ± 0.00054**
M. calidus	***M. ortus***	0.00074	0.00366 ± 0.00147**	0.00788 ± 0.00219**
M. calidus	***M. pumilus***	0.00187	0.00648 ± 0.00046**	0.00662 ± 0.00172**
M. calidus	***M. unicolor***	0.00123	0.00334 ± 0.00086**	0.00628 ± 0.00255**
M. ortus	***M. pumilus***	0.00077	0.00840 ± 0.00062**	0.00184 ± 0.00110**
M. ortus	***M. unicolor***	0.00198	0.00287 ± 0.00054**	0.00242 ± 0.00084**
M. pumilus	***M. unicolor***	0.21329	0.28691 ± 0.03521**	0.24599 ± 0.03617**

Symbols: ** ecological niches are significantly (** $P \leq 0.01$) more similar or different than expected by chance. Abbreviations: NS, non-significant; SD, standard deviation.

Based on the results of integrative taxonomic studies, three taxa belong to this subgroup: two complexes (*Merodon aureus* complex and *M. unicolor* complex) and one species *M. pumilus* Macquart in Lucas, 1849.

MERODON AUREUS COMPLEX

In this study, we describe geometric morphometric and molecular evidence that support the presence of three independent species in the *Merodon aureus*

KEY FOR TAXA FROM *MERODON AUREUS* SUBGROUP *SENSU* ŠAŠIĆ ET AL. (2016)

1. Complete body pile whitish, except few black ones on frons.....*Merodon unicolor* complex
1'. At least eye pile black in upper half.....2
2. Eye contiguity in males longer than 20 ommatidia, about as long as vertical triangle (Fig. 12A); in female ocellar triangle equilateral (Fig. 13A) or isosceles, if isosceles then two lateral sides longer than basal .....*Merodon aureus* complex
2'. Eye contiguity in males short, between 5 and 10 ommatidia, about 2× shorter than length of vertical triangle (Fig. 12C); in female ocellar triangle isosceles, two lateral sides shorter than basal (Fig. 13B).....*Merodon pumilus*

complex: *M. aureus*, *M. calidus* and *M. ortus*, all with distinct and remote distribution, except sympatric populations of *M. aureus* and *M. calidus* on Stara Planina (Serbia).

MERODON AUREUS FABRICIUS, 1805, STAT. REV.

Merodon aeneus Megerle in Meigen, 1822, synon. nov.

Merodon aureus B in Milankov *et al.* (2008).

Redescription: MALE (Figs 10, 11, 12A, B): Length of body 6–10 mm, of wing 6–8 mm (N = 120). *Head (Figs 11A, C, 12B)*: Antenna brown; basoflagellomere reddish-brown to dark-brown, 1.3–1.5 times longer than pedicel [length of basoflagellomere as on fig. 5 in Marcos-García *et al.* (2007)], dorsal margin concave between the arista and the apex, apex rounded; arista yellow basally, as long as pedicel and basoflagellomere together; face and frons shiny black with olive lustre, covered with long pale-yellow pile and indistinct scarce brownish microtrichia, most visible along eye margin; ventral part of face bare, with black lustre; vertical triangle isosceles, shiny black, predominantly covered with long, pale pile, except at anterior end with black ones; eye contiguity more than 20 ommatidia long; ocellar triangle equilateral; eye pile long, black in the upper half or more and lower corner, paler between; occiput shiny, silver-green, covered with whitish microtrichia and pale-yellow pile. *Thorax (Fig. 11A, B, D)*: Mesonotum brown with olive-green reflections, rough punctate, covered with long, dense, erect yellow to orange pile; scutum with three weak vittae of dark brown microtrichia; posterior anepisternum, anepimeron and dorsal part of katepisternum with long yellow pile. *Wing:* Hyaline, with dark-brown veins; calypteres brownish; halteres with brown pedicel and dark brown capitulum. *Legs:* Femora black with brown apex; pile on pro- and mesofemur predominantly yellow, except black pile medially; metafemur predominantly covered with yellow pile, except short, black ones in the apical quarter medially; tibiae and tarsi black, except dark brown basis of tibiae, covered with yellow pile with some intermixed black ones; metatrochanter with inner spine ending in two angular points (one corner more protruded). *Abdomen (Fig. 11A, E)*: Oval, slightly longer than mesonotum; black with olive-green reflections; terga completely covered with yellow to orange pile; sterna shiny black, covered with long, light yellow pile. *Male terminalia:* Similar to all other species of the *M. aureus* group (Fig. 10). *FEMALE (Figs 13A, 14)*: Similar to the male except for normal sexual dimorphism. *Head:* Frons shiny black; vertex mostly covered with black pile, except for posterior end covered with yellow ones. *Legs:* Metatrochanter without spine. *Abdomen:* Shiny black, with pairs of white microtrichose fasciae on terga 2–4; on tergum 2 these fasciae are subparallel to the anterior margin

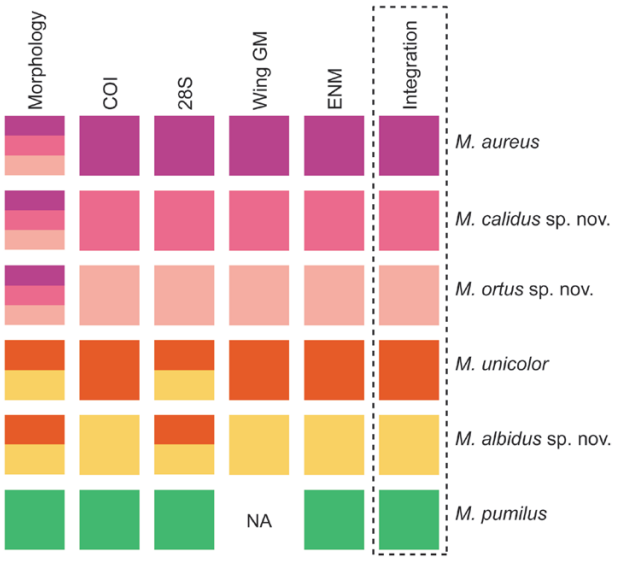

Figure 6. Schematic representation of the results of our integrative taxonomic delimitation of species within the *Merodon aureus* subgroup. Each species complex is represented by a different colour, with species belonging to the same complex being represented by shades of the same colour. Solid boxes indicate successful species delimitation by a particular approach. Multicoloured boxes depict clusters formed by multiple species.

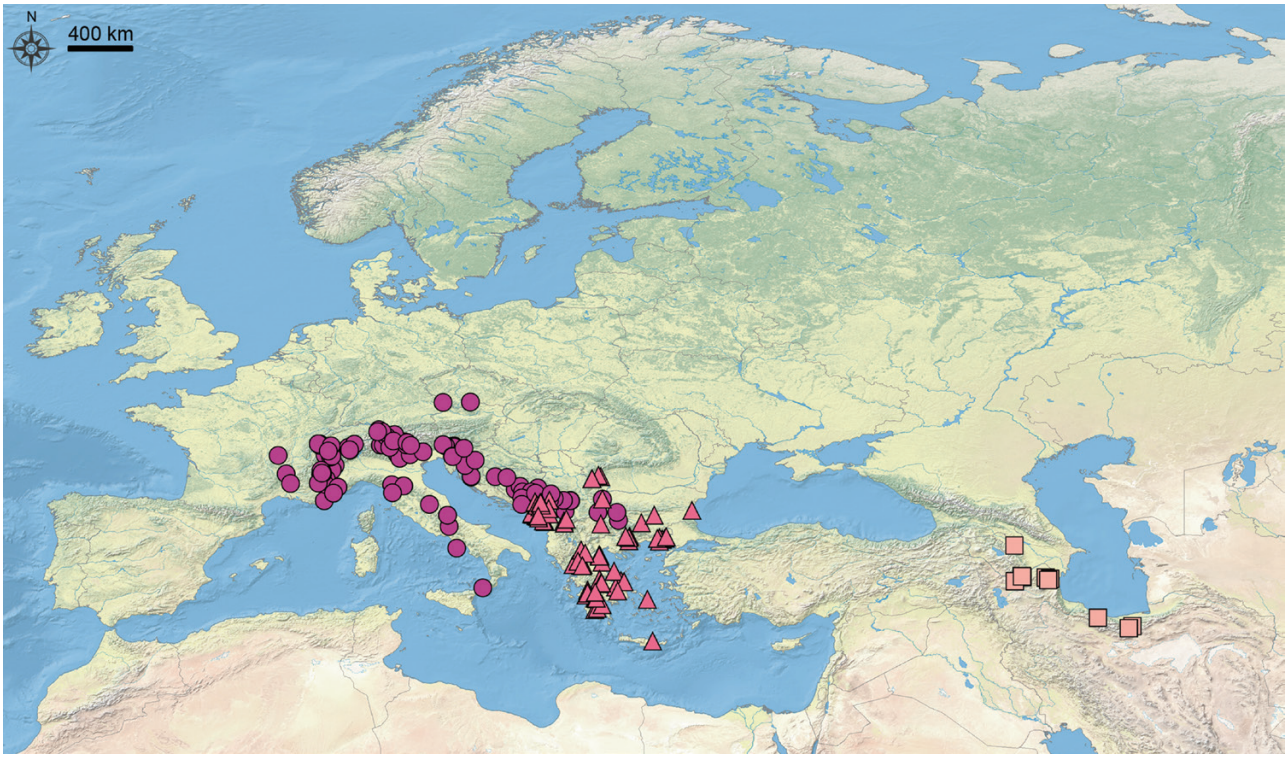

Figure 7. Map of western Palaearctic showing the distribution of species from *Merodon aureus* complex. Symbols: ○ *M. aureus*; Δ *M calidus*; □ *M. ortus*.

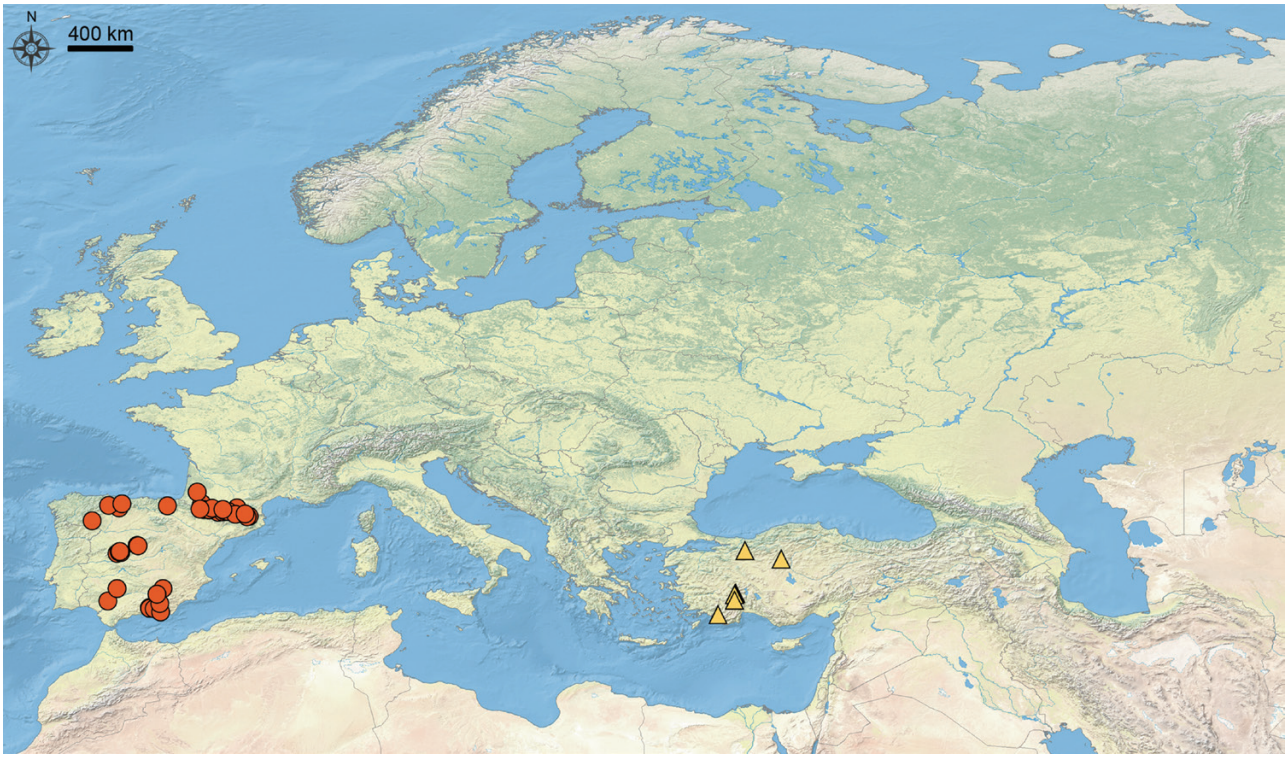

Figure 8. Map of western Palaearctic showing the distribution of species from *Merodon unicolor* complex. Symbols: ○ *M. unicolor*; Δ *M albidus*.

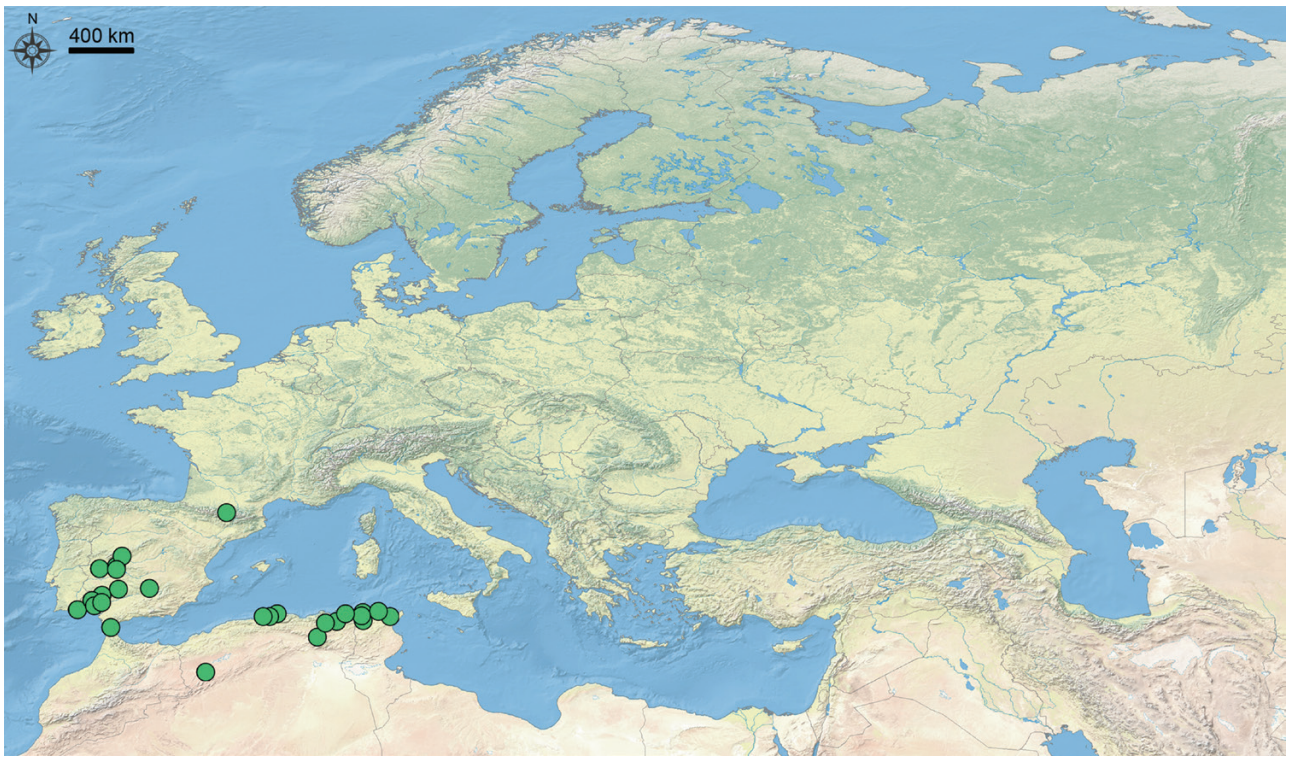

Figure 9. Map of western Palaearctic showing the distribution of *Merodon pumilus*.

of the tergum, whereas on terga 3–4 these fasciae are oblique; terga partly covered with pale pile; black pile present in medial parts of posterior half of tergum 2, all of tergum 3 and on anterior half of tergum 4, except on mictrotrichose fasciae; tergum 5 covered with yellow pile with some intermixed black ones.

Diagnosis: Eye pile black at least in upper half (Fig. 12A, B) (all white in *M. unicolor*); pile on metafemur whitish yellow (Fig. 11B); similar to *Merodon pumilus* from which it can be separated by eye contiguity longer than 16 ommatidia, approximately as long as vertical triangle (eye contiguity in *M. pumilus* 5–10 ommatidia); in female ocellar triangle equilateral or isosceles, if isosceles then two lateral sides longer than basal (Fig. 13A), while in *M. pumilus* isosceles, two lateral sides shorter than basal (Fig. 13B); distance between two posterior ocelli (in Fig. 13A: pink line) comparing distance between posterior ocellus and eye margin shorter in *M. aureus* (in Fig. 13A: yellow line), while in *M. pumilus* distance between two posterior ocelli (in Fig. 13B: pink line) comparing distance between posterior ocellus and eye margin longer (in Fig. 13B: yellow line).

Material examined: Type material: *Syrphus aureus* Fabricius, 1805: 198. Type locality: Germany. Described based on unspecified number of specimens. There are two specimens in the collection considered here as syntypes. Lectotype, designated here, deposited in Copenhagen Museum – ZMUC, with two wings and part of thorax remains on pin, with handwritten label 'aureus' (see Fig. 15). Other syntype is even more destroyed, but still with wings and small part of thorax, designated as paralectotype.

Merodon aeneus Megerle in Meigen, 1822: 367. Type locality: Austria. Type material presumably lost. Neotype (designated here) ♂ AUSTRIA, Lower Austria, Josefsthal, 1856, 48.962132N 15.013034E, Mann leg. (NHMW).

We chose the specimen from Austria as a neotype of *M. aeneus* based on type locality designated in the original description (Austria). The neotype is the property of the Naturhistorisches Museum Wien, Vienna, Austria (NHMW), which maintains a historical collection, with proper facilities for preserving name-bearing types, and that makes them accessible for study.

Notes: Speight (2018) reported: "In the Biosystematic Database of World Diptera (Thompson & Brake, 2005), *Merodon aeneus* is given as a synonym of *M. aureus* Fabricius, but without providing any justification for this supposed synonymy." Speight (2018) also discuss the type of *M. aureus*: "Unfortunately, since Fabricius' description of *M. aureus* is inadequate to decide the identity of the species to which it applies and the

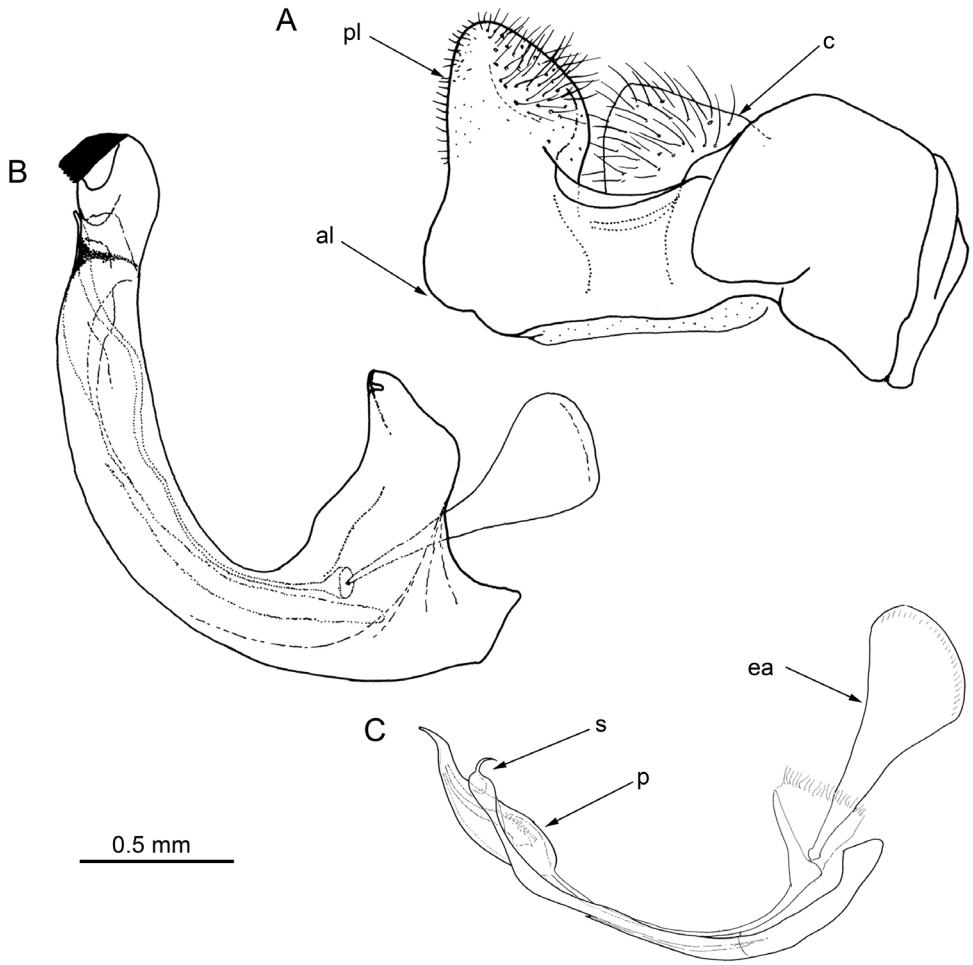

Figure 10. *Merodon aureus*, male genitalia. A, epandrium, lateral view. B, hypandrium, lateral view. C, aedeagus, lateral view. Abbreviations: al, anterior surstyle lobe; c, cercus; ea, ejaculatory apodeme; p, aedeagus; pl, posterior surstyle lobe; s, lateral sclerite of aedeagus.

type material of *M. aureus* is reduced to a remnant comprising, according to Zimsen (1964), 'only wings', there is no basis for establishing this synonymy, unless a neotype can be designated for *M. aureus* (assuming this would be a valid act in the circumstance that there remains a fragment of the original type material, however useless) and a redefinition of *M. aureus* can be provided, that permits its separation from the other *Merodon* taxa to which it is closely related and which have recently been either re-established as species or described as new species (see Marcos-García *et al.*, 2007). No such actions have been taken in any publication produced to date and, until and unless some meaningful basis is established for the claim that *M. aeneus* is a synonym of *M. aureus*, that synonymy is here regarded as unproven. These problems are confounded by the reality that the description of *M. aeneus* cannot be used to separate it from other segregates of the *aeneus* complex now recognised as distinct species and the type material of *M. aeneus* cannot be found."

Descriptions of *M. aureus* and *M. aeneus* are relatively poor with information, but some key characters can be extracted. Fabricius (1805) described males from Germany under the name *Syrphus aureus* and provided some useful characters: small species with orange head and dark antenna, body shining, pile orange (golden), thorax orange, without spots, abdomen black, legs dark, femora black, thickened, with dentate plate. Meigen (1822) described *M. aeneus* based on a single female from Austria with only few characteristics that can be used in the identification of this taxon: metallic dark-green species, with yellow pilosity and brown antenna.

There is only one species morphologically in accordance with both descriptions (*aureus* and *aeneus*) in Central Europe from where the type material from both names originated (Germany, Austria, also in

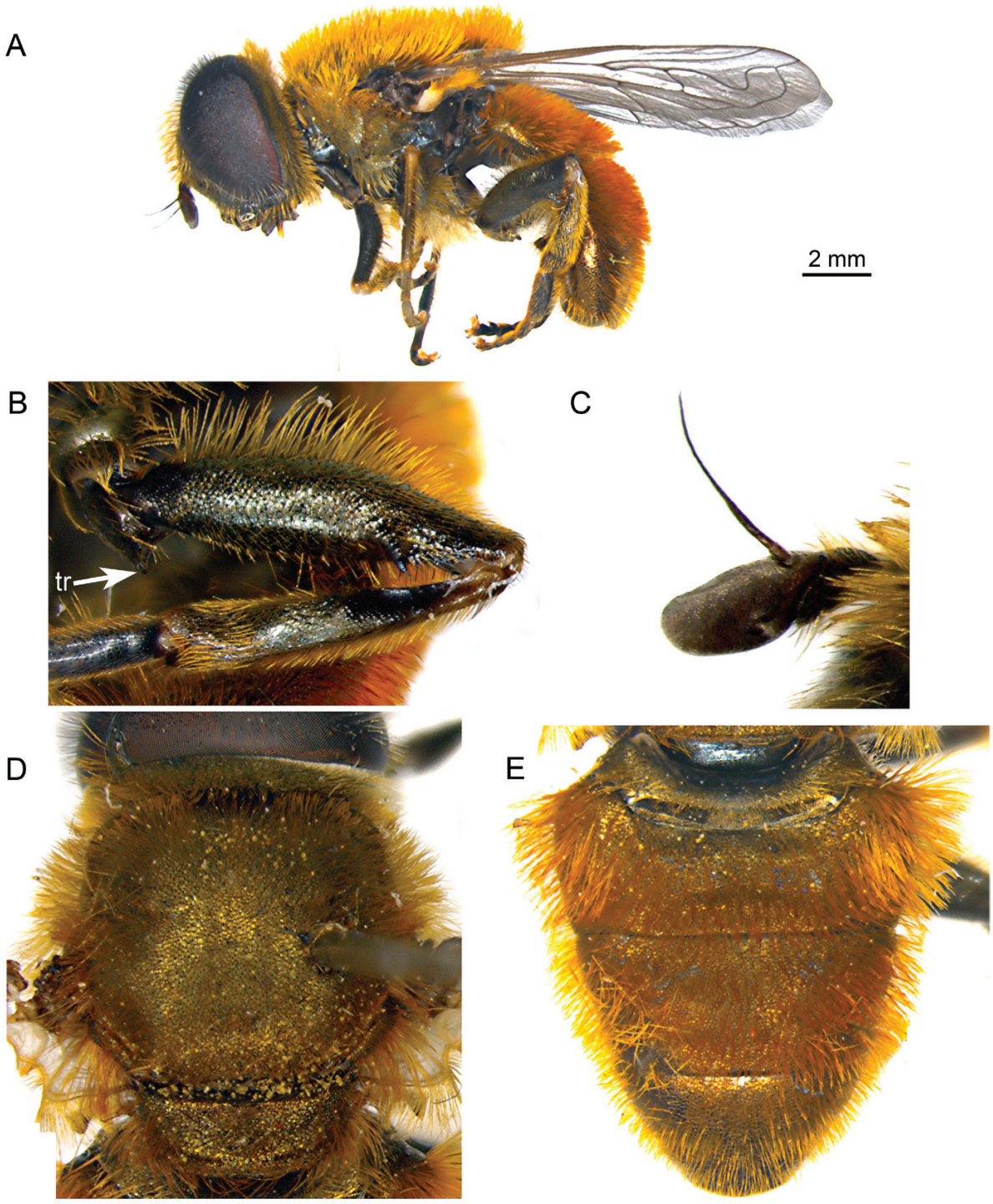

Figure 11. *Merodon aureus*, male. A, body, lateral view 09661 (Switzerland, Simplon Dorf). B, metaleg, lateral view 16008 (Serbia, Zlatar). C, antenna, dorsolateral view 09661 (Switzerland, Simplon Dorf). D, thorax, dorsal view LJ76 (Italy, Trentino). E, abdomen, dorsal view 09626 (Switzerland, Simplon Dorf). Abbreviations: tr, metatrochanter.

Switzerland). Concerning this, we believe that both names refer to the same species. Using the remaining fragment of the *M. aureus* type, we were able to identify this specimen as conspecific with populations cited here under this name. Scutum and coloration of pile perfectly match the *M. aureus* complex and the

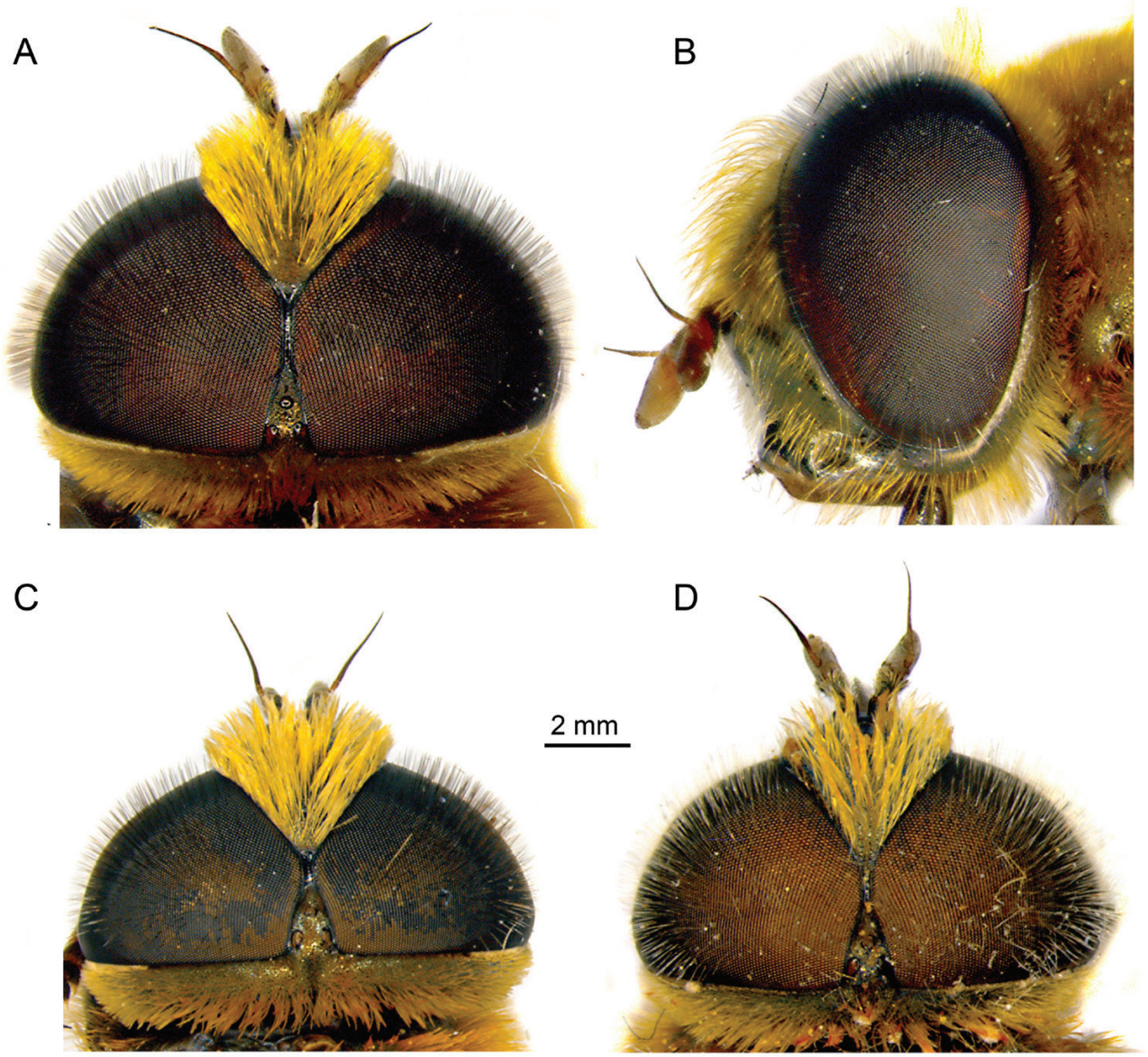

Figure 12. Male head. A, *Merodon aureus*, dorsal view LJ87 (Italy, Trentino). B, *M. aureus*, lateral view LJ87 (Italy, Trentino). C, *M. pumilus*, dorsal view 09437 (Spain, Bolonia 3). D, *M. unicolor*, dorsal view 02945 (Spain, Guadarrama).

wing in our geometric morphometric analyses fit 99% to central European populations.

Among seven species known for Germany, *M. aberrans*, *M. aeneus* (*M. aureus*), *M. armipes*, *M. equestris*, *M. moenium*, *M. ruficornis* and *M. rufus* (Speight 2018), Fabricius (1805) lectotype of *M. aureus* fit to specimens from Germany until now identified as *M. aeneus*. Based on that we propose a designation of neotype for *M. aeneus*, and an establishment of correct synonymy.

We propose here a re-evaluation of a taxon present in high Central European (and Balkans) mountains under the name *M. aureus*, with the name *M. aeneus* as a junior synonym. The taxon presented by Milankov *et al.* (2008) under the name *M. aureus* B, is conspecific with the 'real' *M. aureus*.

Biology and preferred habitat: Preradović *et al.* (2018) described the pupa under the name of *Merodon aureus*. Molecular data presented here reidentified this pupa as an immature stage of *Merodon calidus*. Speight (2018) listed biological data under the name *M. aeneus*. *Preferred environment:* Open ground; unimproved, calcareous montane grassland. *Adult*

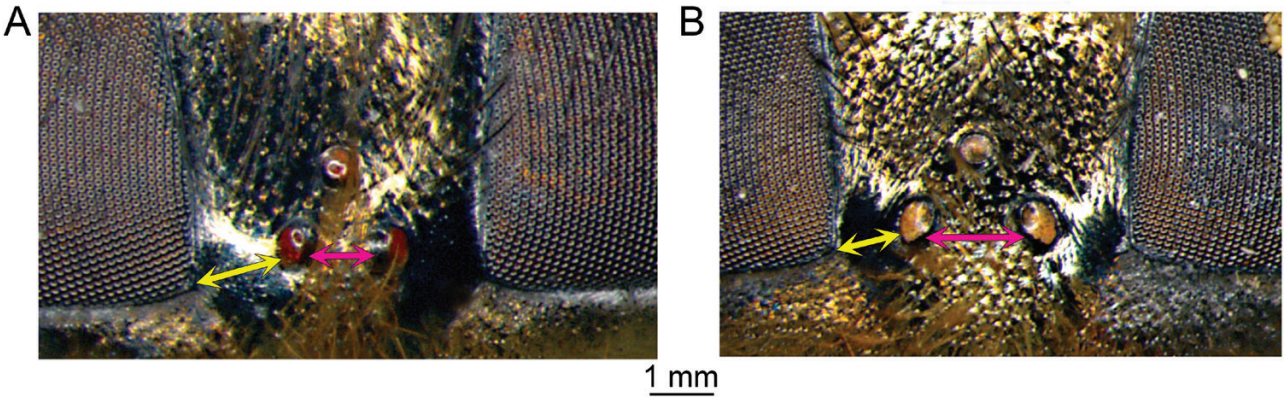

Figure 13. The ocellar triangle of females, dorsal view. A, *Merodon aureus* X81 (Serbia, Kopaonik). B, *M. pumilus* 09438 (Spain, Bolonia 3). Legend: pink arrows – distance between two posterior ocelli; yellow arrows – distance between posterior ocellus and eye margin.

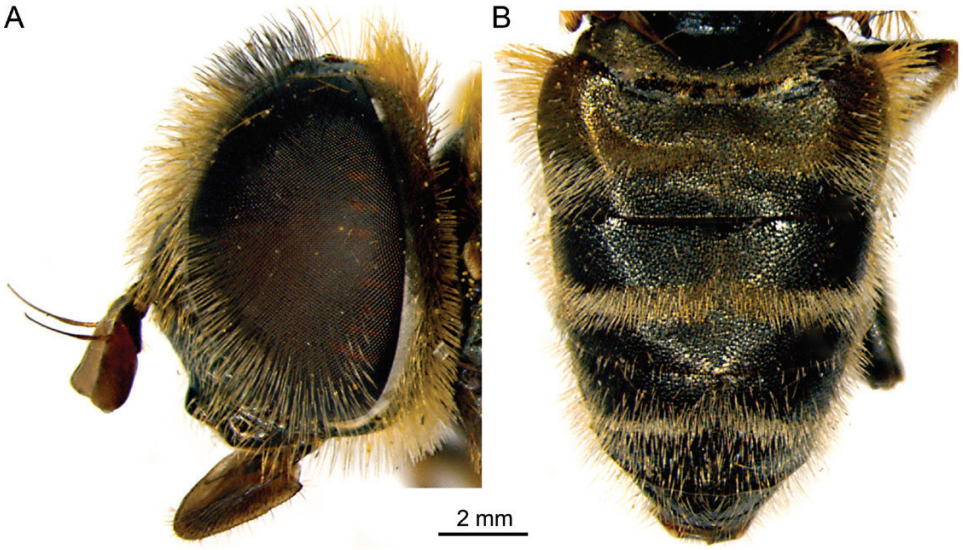

Figure 14. *Merodon aureus*, female. A, head, lateral view 16016 (Serbia, Zlatar). B, abdomen, dorsal view 16017 (Serbia, Zlatar).

habitat and habits: Flies fast and low over ground vegetation in open situations; settles on vegetation, bare ground and stones in the sun. *Flowers visited:* Apiaceae; *Anthericum ramosum* L., *Leucanthemum vulgare* Lam., *Mentha*, *Ranunculus*, *Solidago*, *Taraxacum*. *Flight period:* End of May to August. At higher elevations, the peak is in July/August.

Distribution: Distributed in high Central European (and Balkans) mountains: The Alps in France, Austria, Germany, Switzerland, Italy and Slovenia, the Apennine Peninsula and the Dinaric mountain range in Croatia, Bosnia and Herzegovina, Serbia and Bulgaria. Elevation range starts from sea level up to 2650 m (Figs 7, 16).

MERODON CALIDUS ŠAŠIĆ ZORIĆ *ET AL.* **SP. NOV.**

Merodon aureus A in Milankov *et al.* (2008).

Lsid:urn:lsid:zoobank.org:act:DB0A3C7A-F5A2-48A2-89DA-7E64C3EDA790

Diagnosis: Differs from other species of the *M. aureus* complex based on *COI* gene and 28S rRNA gene sequences divergence (Figs 10, 11) and morphometric character of the wing (Fig. 13B).

Derivatio nominis: The Latin adjective *calidus*, warm or hot, refers to the distribution of new species in the southern mountains on the Balkan Peninsula, which

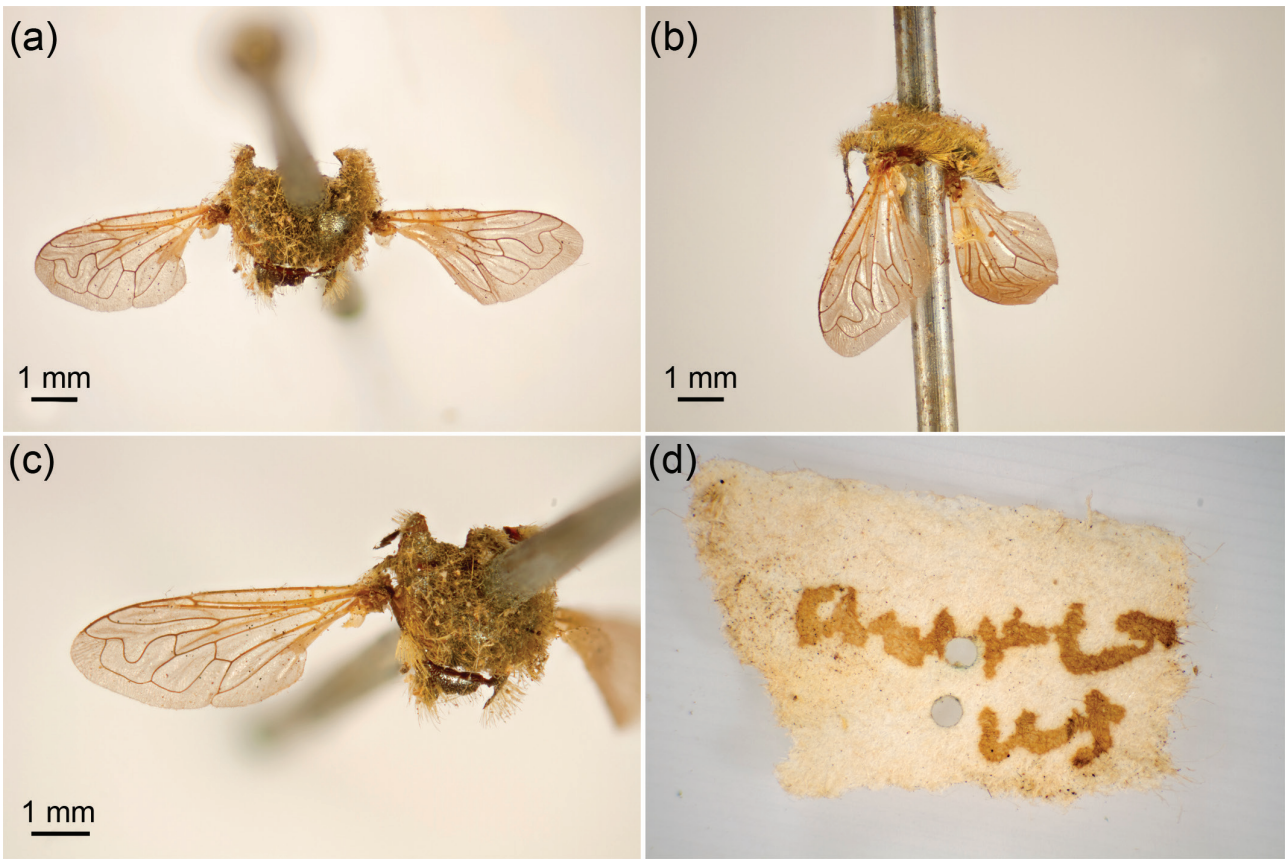

Figure 15. Lectotype of *Merodon aureus*, male. A, part of thorax and wings, dorsal view. B, part of thorax and wings, lateral view. C, right wing used in geometric morphometric analyses. D, original label.

has a warmer climate compared to Alpine and central Balkans mountains habitats of the related *M. aureus*.

Matrial examined: Type material: Holotype ♂, GREECE: Chelmos-Kalavryta ski centre, 06.vi.2017, 38.0067N 22.1948E, A. Vujić, Z. Nedeljković, L. Likov, M. Miličić, T. Tot. leg. (FSUNS, 15975). – Paratypes GREECE: 1♂, Evros, Avas, 28.iv.2000, 40.9318N 25.9024E, van Steenis, Bakker leg. (FSUNS, 03012); 1♀, Evros, Dadia, Lefkimi, Dadia forest, 30.iv.2000, 41.1302N 26.2266E, van Steenis, Bakker leg. (FSUNS, 03011); 1♂, Magnisias, Platania, 05.v.2000, 39.20N 23.29E, Standfuss leg. (D. D. coll., 03014); 3♀♀, 35km NE of Kalambaka, 15.v.2005, Halada leg. (J. H. coll., 18347–18349); 1♂, 1♀, Evros, Mountain Sapka, 15.v.2008, 770 m, 41.145N 25.9094E, de Courcy Williams leg. (FSUNS, G0946, G0947); 1♂, Mountain Pindos, Iznad Hrizopolio, v.2011. 39.601N 21.497E (FSUNS, H55); 1♂, 1♀, Drama, 20–23.v.2011, 41.1504N 24.1522E (FSUNS, I55, I56); 2♂♂, 5♀♀, Drama, Kato Nevrokopi, v.2011, 41.2209N, 23.9669E (FSUNS, I31–I35, I57, I58); 1♂, Mountain Pindos, Katara Pass, 15.v.2011, 39.796N 21.229E (FSUNS, H24); 2♂♂, Mountain Pindos, Desi, 16.v.2011, 976.5 m, 39.5632N 21.3686E (FSUNS, H62, H63); 1♀, Drama, Sidironero 1, 18.v.2011, 41.217N

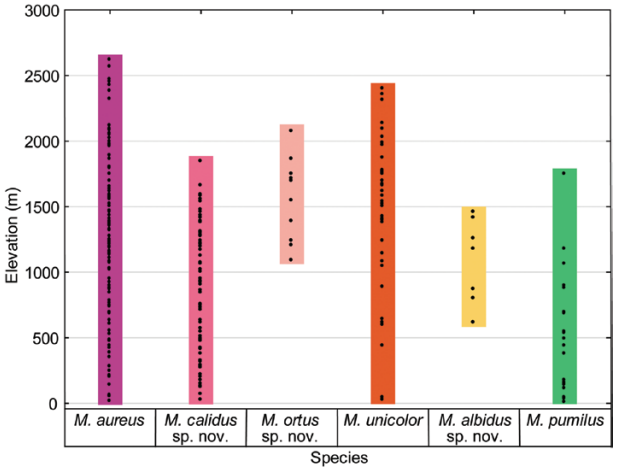

Figure 16. Variability plot of elevation ranges of taxa of the *Merodon aureus* subgroup. Circles represent data on the elevation of the samples.

24.185E (FSUNS, I74); 5♂♂, 2♀♀, Mountain Olympos, Litochoras–Prionia 3, proplanak pored puta, 17.v.2012, 40.106N 22.476E (FSUNS, H84, H85, H91, I10, I2,

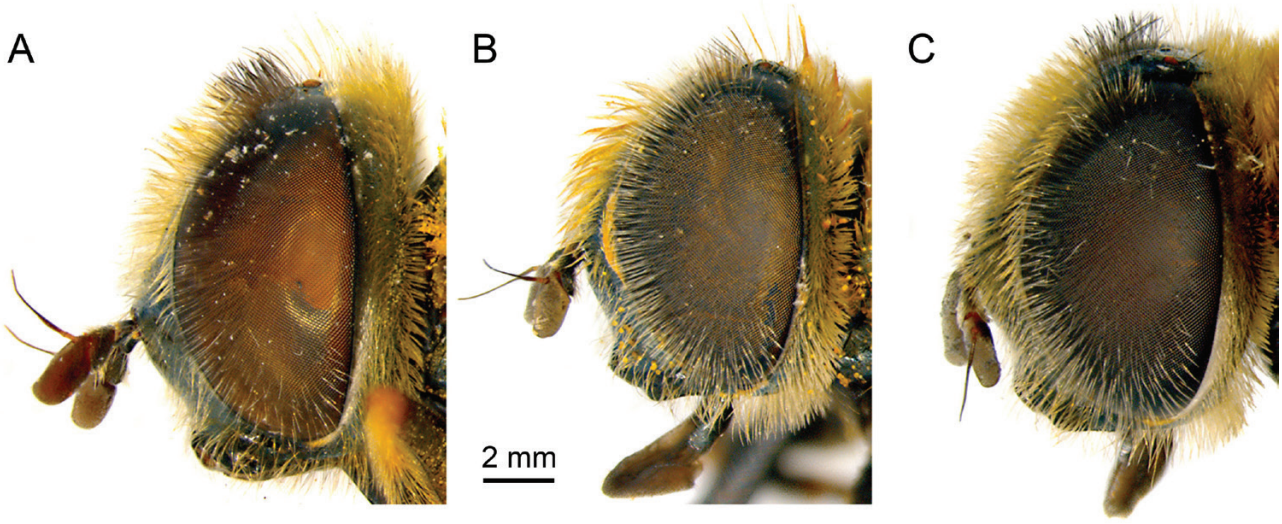

Figure 17. Head, lateral view. A, *Merodon pumilus*, female 03084 (Tunisia, Khathairia). B, *M. unicolor*, male 07300 (Spain, Sierra Nevada). C, *M. unicolor*, female 07303 (Spain, Sierra Nevada).

I3,I5); 26♂♂, 21♀♀, Mega Rema (Dadia N P), Nomos Evros, 07.v.2013, 41.0486N 26.0738E (FSUNS, AI74–AI88, AK29–AK59, AK70); 1♀, Achaia, Near Erimanthos 2, 20.iv.2014, 38.1151N 21.7725E, A. Vujić leg. (FSUNS, 06461); 2♂♂, Achaia, Near Erimanthos 2, 20.iv.2014, 37.9571N 21.7520E, A. Vujić leg. (FSUNS, 06462, 06464); 1♀, Mountain Olympos, Near Litochoro, 21.v.2014, 40.1083N 22.4779E, A. Vujić, J. Ačanski leg. (FSUNS, 06498); 1♂, Mountain Olympos, Moni Agiou Dionisiou, 21.v.2014, 40.1127N 22.4688E, A. Vujić, J. Ačanski leg. (FSUNS, 06509); 1♂, 4♀♀, Lamia, Ano Mpralos, 21.v.2014, 38.7357N 22.4525E, A. Vujić, J. Ačanski leg. (FSUNS, 06511, 06513–06516); 1♀, Achaia, Near Erimanthos 2, 22.5.2014, 37.9571N 21.7520E, A. Vujić leg. (FSUNS, 06688); 1♂, 4♀♀, Ilia, Near Panopoulos, 22.v.2014, 37.8421N 21.6623E, A.Vujić, J. Ačanski leg. (FSUNS, 06523, 06524, 06526–06528); 1♂, Laconia, Karyes, 25 km N from Sparta, 23.v.2014, 37.3041N 22.4210E, A. Vujić, J. Ačanski leg. (FSUNS, 06534); 2♀♀, Arcadia, Between Tripolis and Sparta, 23.v.2014, 37.3041N 22.4210E, A. Vujić, J. Ačanski leg. (FSUNS, 06580, 06581); 1♂, Mountain Mainalo, above Kardaras, 24.v.2014, 1640 m, 37.6597N 22.2598E, A. Vujić, J. Ačanski leg. (FSUNS, 06590); 6♂♂, Mountain Mainalo, ski centre, 24.v.2014, 1550 m, 37.6460N 22.2668E, A. Vujić, J. Ačanski leg. (FSUNS, 06637, 06639, 06644, 06647–06649); 2♂♂, 3♀♀, Arcadia, Kardaras, 24.v.2014, 1108 m, 37.6264N 22.2907E, A. Vujić, J. Ačanski leg. (FSUNS, 06606, 06613, 06599, 06600, 06609); 1♂, 3♀♀, Chelmos-Kalavryta ski centre, 06.vi.2017, 38.0067N 22.1948E, A. Vujić, Z. Nedeljković, L. Likov, M. Miličić, T. Tot leg. (FSUNS, 15976–15979); 1♂, near Mainalon, Ski centre, 07.vi.2017, 37.6534N 22.2600E, A. Vujić, Z. Nedeljković, L. Likov, M. Miličić, T. Tot leg. (FSUNS, 15705); 1♂, Chelmos-Kalavryta ski centre, 08.vi.2017, 38.0067N 22.194826E, A. Vujić, Z. Nedeljković, L. Likov, Miličić M., Tot T. leg. (FSUNS, 15970); 1♂, 1♀, Euboea, near Dasos Stenis, 09.vi.2017, 38.6005N 23.8670E, A. Vujić, Z. Nedeljković, L. Likov, M. Miličić, T. Tot leg. (FSUNS, 15879, 15880); MONTENEGRO: 4♂♂, Orjen (Orijen), 01.vi.2008, 42.5691N 18.5441E, A. Vujić leg. (FSUNS, A98, A99, B3, B4); 1♂, Rumija, Oko sredine (deo ka jezeru, uz put), 02.v.2011, 42.112N 19.2173E, A. Vujić leg. (FSUNS, G0243); 1♂, 1♀, Orjen (Orijen), Planinarski dom, 01.vi.2011, 42.5121N 18.5570E (FSUNS, J83, J81); 2♀♀, Orjen (Orijen), Risan, Crkvice, 01.vi.2011, 42.561N 18.630E (FSUNS, J88, J94); 4♂♂, Orjen (Orijen), Vratlo, 01.vi.2011, 42.5104N 18.5590E (FSUNS, J23, J30, J31, J58); 2♂♂, Durmitor, Ka Savinom kuku, 15.vi.2012, 43.1167N 19.0914E (FSUNS, X40, X50); 2♂♂, 2♀♀, Durmitor, Pošćensko jezero, 01–04.vi.2016, 1045 m, 42.9786N 19.0707E, A. Vujić, L. Likov, M. Miličić, N. Veličković leg. (FSUNS, 11826–11829); 2♂♂, 1♀, Južne padine Žiljova, Zatrijebač – K. Korita, 02.vi.2016, 42.5232N 19.5381E, S. Malidžan leg. (PMCG, 16506, 16509, 16505); 21♂♂, 1♀, Plužine, Pejovic's land, 20.v.2017, 43.027N 18.845E, A. Vujić, Z. Markov, S. Popov, M. Ranković, A. Šebić leg. (FSUNS, 17780–17795, 17797–17802); 1♂, Vojnik, Vioč ka vrhu, 14.vi.2017, 1447 m, 42.9251N 19.0199E, S. Malidžan leg. (PMCG, 16498); 2♂♂, 5♀♀, Lovćen, Lovćen 1, 17.v.2018, 42.3830N 18.8984E, A. Vujić, A. Šebić, M. Ranković leg. (FSUNS, 18996, 19003–19005, 19007, 19010, 19013); 3♂♂, 1♀, Lovćen, Lovćen 2, 17.v.2018, 42.3711N 18.8715E, A. Vujić, A. Šebić, M. Ranković leg. (FSUNS, 18947, 18955, 18969, 18975); 1♀, Lovćen, Lovćen 4, 18.v.2018, 42.3664N 18.8926E, A. Vujić, A. Šebić, M. Ranković leg. (FSUNS, 18984); SERBIA: 6♂♂, 7♀♀,

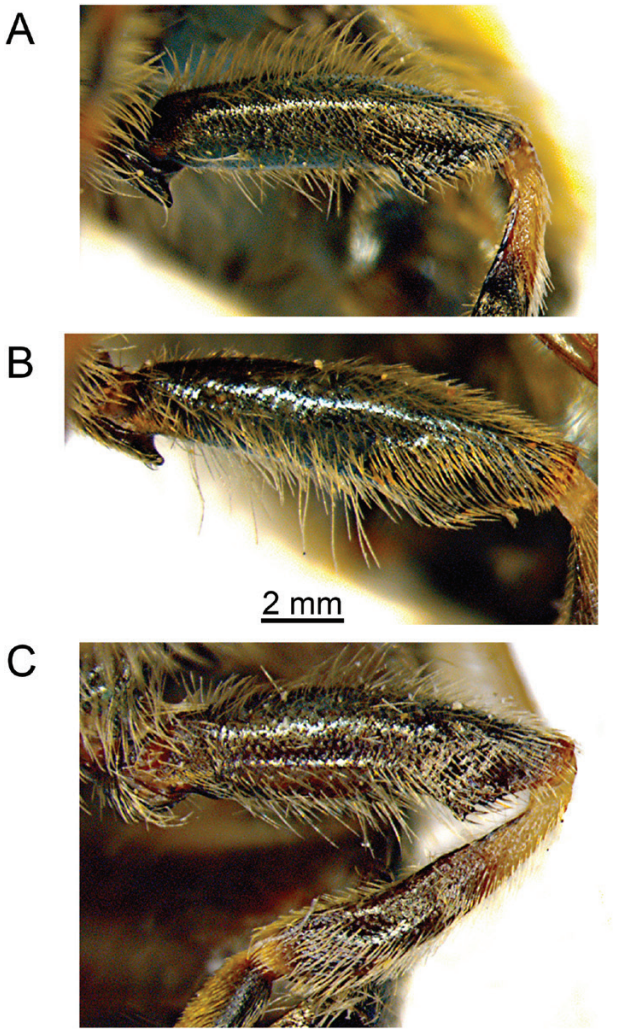

Figure 18. Metafemur, lateral view. A, *Merodon pumilus*, male 03092 (Tunisia, Khathairia). B, *M. unicolor*, male 04856 (Spain, Andalusia). C, *M. unicolor*, female 02950 (Spain, Cofinal).

Đerdap, Ciganski potok, 07.v.2010, 44.5410N 22.0202E, A. Vujić leg. (FSUNS, A81, A82, A84–A90, A95–A97, D62); 1♂, Đerdap, Ciganski potok, iv.2011, 44.541N 22.020E, A. Vujić leg. (FSUNS, G65); 7♂♂, 6♀♀, Đerdap, Ciganski potok 2, iv.2011, 44.5410N 22.0202E, A. Vujić leg. (FSUNS, G43, G46, G48, G49, G51, G57, G58, G80–G82, G85, G87, G88); 1♂, Stara Planina, Babin zub, 21.vi.2009, 43.3740N 22.6201E, A. Vujić leg. (FSUNS, G1667); 6♂♂, Stara Planina, Babin zub, 21.vi.2012, 43.3740N 22.6201E, A. Vujić leg. (FSUNS, U79, U80, U81, U83, U85, U89, U94, U99, W13).

Distribution: Distributed on southern parts of Balkan Peninsula, in Greece, Montenegro, North Macedonia, Albania, Bulgaria and Serbia. Elevation range is variable, between sea level and 1850 m (Fig. 16).

MERODON ORTUS ŠAŠIĆ ZORIĆ *ET AL.* **SP. NOV.**

Lsid:urn:lsid:zoobank.org:act:9C9789AF-D797-4EF4-AE9F-D52C1F85CAC4

Diagnosis: Differs from other species of the *M. aureus* complex based on *COI* and 28S rRNA gene sequences divergence (Figs 10, 11) and morphometric character of the wing (Fig. 13B).

Derivatio nominis: The Latin noun *ortus*, east or origin, refers to the distribution of species in the Middle East. It should be treated as a noun in apposition.

Material examined: Type material: Holotype ♂, IRAN: Qaradagh forest, 05.viii.2012, 1940 m, 38.8638N 46.8331E, Khaganinia leg. (IHCMM, 10291). – Paratypes AZERBAIJAN: 11♂♂, 2♀♀, Caucasus, Talysch (mountain range), 1885, 38.7000N 48.3E, Mik leg. (NHMW, 03025, 03026, 05739–05749); 1♀, Lerik, Lerik, 13.vi.1996, 38.7752N 48.4152E, A. Vujić leg. (FSUNS, 03023); 1♂, Yardymli, Avash, 15.vi.1996, 1200/1500 m, 38.8333N 48.1666E, Hauser leg. (M. H. coll., 03022); 1♂, Caucasus, Ganja (Elizavetpol), Mik leg. (03024, NHMW); IRAN: 1♀, Mazandaran, Kelardasht, Tuydareh, 24.v.2003, 1400 m, 36.5166N 51.1666E, Gilasian leg. (HMIM, 03021); 1♀, Mazandaran, Anarum, 08.vi.2006, 1400, 36.0369N 53.1597E, Gilasian leg. (HMIM, 03037,); 1♂, 4♀♀, Tehran, Veresk, 08.vi.2006, 1750 m, 35.9177N 52.9597E, Gilasian leg. (HMIM, 03034–03036, 03038, 03039); 1♂, Chichekli forest, 20.viii.2009, 1222 m, 38.6337N 46.3927E, 1222 m, Khaganinia leg. (IHCMM, 10267); 1♂, Qaradagh forests, 05.viii.2012, 2021 m, 38 53.815N 46 48.800E, Khaganinia leg. (IHCMM, 10287); 1♀, Qaradagh forest, 05.viii.2012, 1313 m, 38 55.601N 46.932E, Khaganinia leg. (IHCMM, 10288); 2♂♂, 1♀ (FSUNS, 03018–03020).

Distribution: Distributed in the Caucasus of Azerbaijan and high mountains of Iran south of the Caspian Sea at elevations between 1050 and 2100 m (Fig. 16).

MERODON UNICOLOR COMPLEX

The complex comprises two species: *Merodon unicolor* and *M. albidus*. The first is known from the Pyrenees and the Iberian Peninsula. The second is a new species discovered using molecular and morphometric data and is found in Anatolia.

MERODON UNICOLOR STROBL IN CZERNY & STROBL, 1909

Diagnosis: Complete body pile whitish, except few black ones on frons; eye pile white (Figs 12D, 17C) (black at least in upper half in *M. aureus* and *M. pumilus*); pile on metafemora whitish (Fig. 18B, C);

eye contiguity between 15 and 20 ommatidia, slightly shorter than length of vertical triangle (Fig. 12D).

Material examined: Type material: *Merodon aeneus unicolor* Strobl in Czerny & Strobl, 1909: 203. Type locality: Spain. *Merodon unicolor* was described as a variety of *M. aeneus* Megerle in Meigen, 1822 from a single male. Holotype♂, SPAIN, Escorial 'v. *unicolor* m / Spain. / Typus' (NMBA).

Biology and preferred habitat: Marcos-García *et al.* (2007) and Speight (2018) revealed some biological data. *Preferred environment:* Forest/open ground; well-drained, non-calcareous, montane and subalpine unimproved grassland; hedgehog heath; open, grassy areas in montane *Betula* and *Pinus* forest, up to and including *Pinus uncinata* forest in the Pyrenees. *Adult habitat and habits*: Fast-flying, at up to 1.5 m from the ground, through and around tall ground vegetation. *Flowers visited: Anthemis mixta* L. *Flight period:* April to September.

Distribution: Distributed in south-western Europe across the Iberian Peninsula: the Pyrenees in France, Andorra and Spain, and mountainous areas in Spain. The elevation range is from sea level to 2400 m (Figs 8, 16).

MERODON ALBIDUS ŠAŠIĆ ZORIĆ *ET AL.* **SP. NOV.**

Lsid:urn:lsid:zoobank.org:act:031C530F-28A2-4C79-9A60-6C865C9A168E

Diagnosis: Differs from *M. unicolor* based on *COI* gene sequences divergence (Fig. 11) and morphometric character of the wing (Fig. 13C).

Derivatio nominis: The Latin adjective *albidus*, white, refers to white pilosity of the body of this species.

Material examined: Type material: Holotype ♂, TURKEY: Isparta, Keçiborlu, Gülköy, 22.vi.2015, 1502 m, 37.9683N 30.2594E, A. Vujić, Hayat, Gök, Uzal leg. (EMIT, 09932). – Paratypes TURKEY: 1♂, Bolu, above Göynük, 17.v.1960, 610 m, 40.4002N 30.7883E, Guichard, Harvey leg. (BMNH, 04358); 1♀, Ankara, Ankara, 24.vi.1984, 39.9272N 32.8644E, Lucas leg. (NBCN, AM-05-109); 3♀♀, Ankara, 10 km from Ankara, 05.vi.1988, 39.9272N 32.8644E, Warncke leg. (NBCN, AM-05-108, AM-05-113); 1♀, Muğla, 16 km NNW from Üzümlü, brooklet near Kukpunar, 28.v.2000, 1350 m, 36.7336N 29.2333E, Smit leg. (J. S. coll., 04063); 5♀♀, Isparta, Keçiborlu, Gülköy, 22.vi.2015, 1502 m, 37.9683N 30.2594E, A. Vujić, Hayat, Gök, Uzal leg. (EMIT, 09931, 09933, 09934, 09935, 09936); 2♀♀, Isparta, Keçiborlu, Kavak–Kapanlı Arası (II), 22.vi.2015, 1500 m, 37.9269N 30.1908E, A. Vujić, Hayat, Gök, Uzal leg. (EMIT, 09939, 09940,); 1♀, Isparta, Keçiborlu, Kozluca–Gülköy Yolu, 22.vi.2015, 1522, 37.8981N 30.1830E, A. Vujić, Hayat, Gök, Uzal leg. (EMIT, 09938); 1♀, Burdur, Burdur Aziziye Yolu—1 -, 02.vii.2015, 1300 m, 37.5622N 30.1780E, A. Vujić, Hayat, Uzun, Uzal, Gök, Demirözer leg (EMIT, 09937).

Distribution: Mountainous species, distributed in south-western and north-western Turkey (Fig. 7). According to available data, the elevation range is from 610 to 1522 m (Fig. 16).

SPECIES NOT PART OF A COMPLEX

MERODON PUMILUS MACQUART IN LUCAS, 1849

Diagnosis: Eye pile black at least in upper half; eye contiguity in male short, between 5 and 10 ommatidia, about two times shorter than length of vertical triangle (Fig. 12C); female of *M. pumilus* (Fig. 17A) similar to *M. aureus*, but differs with shorter distance between posterior ocellus and eye margin (in Fig. 13B: yellow line) comparing distance between two posterior ocelli (in Fig. 13B: pink line), while in *M. aureus* distance between two posterior ocelli (in Fig. 13A: pink line) comparing distance between posterior ocellus and eye margin (in Fig. 13A: yellow line) shorter; ocellar triangle isosceles, two lateral sides shorter than basal (Fig. 13A); pile on metafemora pale (Fig. 18A).

Material examined: Type material: *Merodon pumilus* Macquart in Lucas, 1849: 466. Type locality: Algeria, Constantine. *Merodon pumilus* was described from a single female. Holotype: ♀, ALGERIA, Constantine, '*pumilus* Macq. sp. nova / Type' (MNHN).

Biology and preferred habitat: Marcos-García *et al.* (2007) and Speight (2018) listed some biological data. *Preferred environment:* Forest/open ground; open areas in thermophilous *Quercus* forest and evergreen oak forest; maquis and matorral; xeric grassland. *Adult habitat and habits:* No data. *Flowers visited:* Apiaceae; *Anthericum ramosum*, *Leucanthemum vulgare*, *Mentha*, *Ranunculus*, *Solidago*, *Taraxacum*. *Flight period:* April to June.

Distribution: Distributed in north-western parts of Africa (the Atlas mountain range in Morocco, Algeria and Tunisia) and south-western parts of Europe (Portugal and Spain). According to available data, the elevation range is from sea level to 1700 m (Figs 9, 16).

DISCUSSION

Resolving species complexes

Cryptic speciation within the *M. aureus* and *M. unicolor* species complexes is supported here by multiple lines of evidence. The species within these complexes differ based on *COI* sequence variability, which can be clearly visualized in our MP and ML trees and confirmed by pairwise average uncorrected p distances among species. These distance values (0.8–2.5% within the complexes) are in the range of values (0.3–2.5%) recorded for cryptic, closely-related hoverfly species (Marcos-García *et al.*, 2011; Vujić *et al.*, 2013b; Nedeljković *et al.*, 2015; Popović *et al.*, 2015; Šašić *et al.*, 2016; Radenković *et al.*, 2018b). The average uncorrected p distance between the species within these complexes and *M. pumilus* is ~8% (Table 1), indicating that *M. pumilus* is clearly molecularly differentiated, which is also strongly supported by our *COI* trees. The strict consensus MP and the ML *COI* gene tree topologies are identical, resolving species into distinct reciprocally monophyletic clades that are strong evidence of differentiation. The relatively low bootstrap supports for *M. aureus* (ML – 68) and *M. calidus* (MP – 61, ML – 62) may be due to sample size. Bootstrap support decreases with increased taxon sampling and also depends on the number of characters assessed (i.e. those supporting the clade of interest and the entire dataset) (Soltis & Soltis, 2003).

Additional evidence for species diversification in the *M. aureus* species complex is provided by the 28S rRNA gene sequences. Although rarely used at the species level due to its low divergence rate, 28S rRNA gene is also successfully applied in other insect species groups, such as tropical water beetles (Coleoptera: Dytiscidae, Hydrophilidae) and dung beetles (Scarabaeidae) (Monaghan *et al.*, 2005), hydropsychidae caddisflies (Trichoptera: Hydropsychidae) (Zhou *et al.*, 2007) and wasps of the *Encyrtus sasakii* Ishii complex (Hymenoptera: Encyrtidae) (Wang *et al.*, 2016). Additionally, 28S rRNA gene sequences have proven informative for species delimitation in the *M. luteomaculatus* complex (Radenković *et al.*, 2018b) and the *M. nanus* group (Kočiš Tubić *et al.*, 2018). In this study, the three species within the *M. aureus* complex can be clearly resolved using this molecular marker. *Merodon pumilus* also possesses a unique 28S rRNA genotype. However, species of the *M. unicolor* complex (*M. unicolor* and *M. albidus*) share the same 28S rRNA genotype.

In accordance with molecular divergence, the species from the *M. aureus* and *M. unicolor* species complexes are also highly and significantly divergent based on wing geometric morphometry. The taxonomic importance of this trait has been proven for interspecific differentiation of species from the *M. aureus* group (*cinereus* subgroup: Šašić *et al.*, 2016; *bessarabicus* subgroup: Radenković *et al.*, 2018b), as well as for other *Merodon* species groups (*nigritarsis* group: Ačanski *et al.*, 2016; *nanus* group: Kočiš Tubić *et al.*, 2018) and hoverfly genera *Eumerus* Meigen, 1822 (Chroni *et al.*, 2018), *Chrysotoxum* Meigen, 1803 (Nedeljković *et al.*, 2013, 2015) and *Pipiza* Fallén, 1810 (Vujić *et al.*, 2013b). Importantly, geometric morphometric results were in accordance with molecular data in all of these previous studies.

Besides the highly significant wing-shape differences among species in the *M. aureus* complex, we also observe an interesting wing-shape pattern among male specimens. The sympatric species *M. aureus* and *M. calidus* have the most divergent wing shapes, whereas the most similar wing shape is between *M. aureus* and the geographically distant species *M. ortus*. The observed differences in mean wing shape are mainly associated with broadness of the central and apical parts of the wing. Similar findings have been reported for *M. unicolor* and *M. albidus*, as well as among species from the *M. atratus* and *M. luteomaculatus* complexes (Šašić *et al.*, 2016; Radenković *et al.*, 2018b). Mean wing-shape differences between *M. aureus* and *M. calidus* may primarily be due to their sympatry and synchronic coexistence on Stara Planina Mountain (Serbia) considering that, apart from flight ability, wing shape influences male species-specific courtship song (Cowling & Burnet, 1981; Stubbs & Falk, 1983; Routtu *et al.*, 2007; Menezes *et al.*, 2013; Outomuro *et al.*, 2013; Sacchi & Hardersen, 2013). This same pattern has previously been reported between sympatric species of the *M. nanus* group (Kočiš Tubić *et al.*, 2018).

Additional support for our species delimitation was provided by the results of population-level morphometric analysis of wing shape, in which all conspecific populations were grouped together. Moreover, clustering of species in species complexes is noticeable. Here, it is important to emphasize that sympatric populations of *M. aureus* and *M. calidus* from Stara Planina were found to be remarkably different in terms of wing shape.

The spatial distribution of species of the *M. aureus* subgroup indicates allopatry between most species, except for the *M. unicolor–M. pumilus* and *M. aureus–M. calidus* pairs. However, we find little evidence of niche overlap between any pairs of taxa, suggesting that each taxon occupies a distinct environmental niche. Thus, our niche similarity test rejects the null hypothesis that the environmental niches of investigated species pairs are similar, instead indicating that they are environmentally divergent, which perhaps plays an important role in explaining both the origin and ongoing differentiation of species in this closely related group of hoverflies. The only

exception to this outcome was the *M. aureus*–*M. calidus* species pair, which presented significant evidence of niche conservation. This result indicates that this latter species pair could occupy each other's habitat, as is the case at Stara Planina where they are sympatric. Thus, we can conclude that the diversification of these two species is not a consequence of environmental conditions.

Evidence of mtDNA introgression

Discordance between mitochondrial *COI* gene trees and nuclear 28S genotypes with regard to placement of particular specimens from Stara Planina (AU695–AU697, AU699, AU169) and Kamena gora (AU1523) can be explained by mtDNA introgression from *M. aureus* to *M. calidus*. The high level of 28S rRNA gene divergence between *M. aureus* and *M. calidus* is unusual between closely related species and, accordingly, we believe that this gene is less likely to be introgressed in this particular case. It is generally accepted that mtDNA introgression is more common than introgression of nuclear genes, due to the mitochondrial genome not being linked to the nuclear one and, thus, not being linked to genes contributing to reproductive isolation (Barton & Jones, 1983; Harrison, 1989; Harrison & Larson, 2014).

We think that asymmetric introgressive hybridization, detected on Stara Planina and Kamena gora, is a consequence of a secondary contact after a longer period of allopatric diversification between *M. aureus* and *M. calidus* (a detailed explanation of changes in spatial distribution is provided below). This introgressive hybridization event upon secondary contact is likely a consequence of undeveloped or partially developed pre-mating barriers between the species that had diverged in allopatry over a long period (Sánchez-Guillén *et al.*, 2016). Our data on geometric morphometry (discussed above) support this hypothesis of secondary contact and co-occurrence on Stara Planina of species from the *M. aureus* species complex. The divergence in male wing shape between *M. aureus* and *M. calidus* is probably a consequence of interspecies reproductive competition upon secondary contact since wing shape influences male species-specific courtship song (Cowling & Burnet, 1981; Stubbs & Falk, 1983; Ritchie & Gleason, 1995; Tauber & Eberl, 2003; Menezes *et al.*, 2013). Competition for the shared territorial and/or signalling space involved in mate attraction and reproduction prompts the evolution of competitive characters (Lipshutz, 2018).

Placement of the *M. calidus* specimen AU713 (of the *M. aureus* species complex) in a cluster with specimens of *M. albidus* (of the *M. unicolor* complex) clade in our *COI* tree also indicates a past introgression event between these two different species complexes. Specimen AU713 was correctly identified and possessed 28S rRNA genotype IV, which is unique for *M. calidus* Despite detecting introgression between *M. calidus* and *M. albidus*, we do not have any records indicating that any of their populations are sympatric. However, it is possible that the species came into contact during Pleistocene range shifts. Post-introgression mutation could also explain the divergence between *M. calidus* specimen AU713 and the *M. albidus* clade whereby haplotypes differentiate upon post-introgression mutation when two species stop exchanging genes, but the species would still be related and nested together within a cluster on a phylogenetic tree if the time since introgression is not long (Funk & Omland, 2003).

Speciation in Pleistocene refugia

Evidence of possible cryptic speciation in southern Europe and adjacent areas, explained in the context of the complex geological history and drastic climate changes during the Pleistocene, is already documented for many insect species (e.g. Borer *et al.*, 2010; Lecocq *et al.*, 2013; Rodrigues *et al.*, 2014; Jaskuła *et al.*, 2016; Schmitt *et al.*, 2016; Martinet *et al.*, 2018) and specifically for hoverflies (e.g. Ačanski *et al.*, 2016; Šašić *et al.*, 2016; Radenković *et al.*, 2018b).

Species of the *M. aureus* complex are generally adapted to high mountain areas and colder climates, but can also be present at lower elevations (from 0 to 2700 m). They correspond to the group of montane species that Schmitt *et al.* (2010) described as being adapted to the forest belt habitat and occur at lower elevations than alpine species. Species currently restricted to high mountains and/or high latitudes probably achieved their maximum range expansion during the Ice Ages, with climate warming during interglacial periods causing range contractions toward higher elevations and latitudes (Schmitt *et al.*, 2010). Range contractions result in spatial fragmentation of species ranges, and disruption of gene flow between isolated allopatric populations, can trigger divergence and, in some cases, speciation in cold-adapted species (Martinet *et al.*, 2018).

The spatial distributions of *M. aureus*, *M. calidus* and *M. ortus* point to the possibility that these species evolved upon isolation of a formerly widespread species in refugia on the Apennine, Balkan and Anatolian peninsulas during the Pleistocene. *Merodon aureus* and *M. calidus* are currently distributed on high mountains of the Apennine and Balkan peninsulas, representing two of the three main refugial centres of Mediterranean species (the other being the Iberian Peninsula) (Schmitt, 2007). We assume that *M. aureus* was primarily distributed on the Apennine Peninsula, although it is also now present in the Alps and on high Dinaric mountains of the north-west Balkans,

whereas *M. calidus* occurs on high oro-Mediterranean mountains of the Balkan Peninsula (i.e. a more southerly distribution). As the climate became more favourable, probably during glacial–interglacial shifts, *M. aureus* likely expanded towards the Alps in the north and to the Balkan Peninsula in the east (even though the Alps to the west still represented an insurmountable barrier for further expansion). Meanwhile, *M. calidus* probably expanded its range from the south to the north of the Balkan Peninsula. During interglacial periods, these populations may have retracted toward the higher elevation areas of the Alps, Apennines and the mountains of the Balkan Peninsula. This pattern of range modification during the Pleistocene was likely repeated a few times to give rise to present species distributions. The third species from this complex, *M. ortus*, is distributed on high mountains around the southern part of the Caspian Sea (Caucasus Mountains and high mountain ranges of Iran) and it is clearly separated geographically from *M. aureus* and *M. calidus*. There is no evidence that this species expanded its range to the west or north, out of Caucasian region. Isolation of Caucasus/Caspian lineages, expressed through high endemicity in this region, has previously been documented in diverse insect groups (e.g. hoverflies: Vujić *et al.*, 2013a; Ačanski *et al.*, 2017; scorpion flies: Dvořák & Ghahari, 2016 and dragonflies: Schneider *et al.*, 2018).

The two species belonging to the *M. unicolor* complex, *M. unicolor* and *M. albidus*, occur at lower elevations than the *M. aureus* species complex. They are more adapted to the warmer Mediterranean climate. *Merodon unicolor* is distributed in the Iberian Peninsula and the Pyrenees, whereas *M. albidus* is present in Anatolia. The ancestral species probably had a wider distribution in southern Europe, but drastic climate changes during the Pleistocene may have resulted in extinction over most of its range, giving rise to the distribution pattern seen today.

Speciation in the *M. aureus* species complex probably occurred during the interglaciations prior to the last Ice Age, assuming that the current interglacial period represents a short time for diversification into separate species (the last glacial, Würm, ended around 11 000 years ago; Berggren, 1972; Ivy-Ochs *et al.*, 2008). It is far more complicated to speculate on divergence times in the *M. unicolor* complex, because p distances based on *COI* gene sequences indicate a similar or higher rate of divergence between the two species within the *M. unicolor* complex compared to these species relative to *M. aureus* and *M. calidus*. Although speciation events can be dated based on *COI* gene sequence divergence and the known evolutionary rate of mitochondrial protein-coding genes (Rutschmann, 2006), diversification of the *M. aureus* subgroup is rather recent and there is evidence of mtDNA introgression, which could result in misinterpretations of the molecular clock, so we have not adopted this approach here.

Merodon pumilus represents a species within the *M. aureus* subgroup, but is distinct from the mentioned species complexes. This species is clearly divergent from the *M. aureus* and *M. unicolor* species complexes based on morphology, molecular data (both *COI* and 28S rRNA gene sequences), geometric morphometry and preferred environmental niches. It is distributed on the Iberian Peninsula and Morocco. This distribution pattern indicates spread across the Strait of Gibraltar; a dispersal route also described for other insect species (e.g. Pinto-Juma *et al.*, 2008; Rodrigues *et al.*, 2014). The Strait of Gibraltar opened ~5.33 Mya and has not been closed since. However, during the Ice Ages, it became narrower due to lower sea levels, which may have facilitated transit (Hewitt, 2011), but as yet, we cannot speculate about the direction of spread of *M. pumilus*, because we have genetic data for only two Moroccan specimens.

CONCLUSION

In this study we resolved nomenclatural issues highlighted by Speight (2018) regarding two names, i.e. *M. aureus* and *M. aeneus*. In the interests of nomenclatural stability, we have designated a neotype for *M. aeneus*, a junior synonym of *M. aureus* that is distributed from Germany through the Alps to the high Balkan mountains. Within the *M. aureus* species group (Fig. 6), we resolved the *M. aureus* subgroup that comprises of two species complexes – the *M. aureus* species complex (*M. aureus*, *M. calidus*, *M. ortus*) and the *M. unicolor* species complex (*M. unicolor*, *M. albidus*) – as well as the species *M. pumilus*. Additionally, we have redefined the pupal stage previously described for *M. aureus* (Preradović *et al.*, 2018) as *M. calidus*. Thus, integration of morphological data with DNA sequence analyses, geometric morphometry of wings, distributional data and environmental niche modelling can enable designation of species complexes and aid species descriptions (Fig. 1).

ACKNOWLEDGEMENTS

The authors thank Mr John O'Brien for the linguistic revision of the manuscript and Thomas Pape and Mikkel Høegh Post from the Natural History Museum of Denmark, Copenhagen for providing photos of the lectotype of *Merodon aureus*. The study was supported by the Ministry of Education, Science and Technological Development, Republic of Serbia, Grant No. 173002, III43002, 451-03-68/2020-14/200358 and 451-03-68/2020-14/200125, and the European Commission, Horizon 2020 project 'ANTARES' (Grant

No. 739570). We also thank TÜBİTAK (The Scientific and Technological Research Council of Turkey) for financial support for the project 213O243 within the scope of which some type specimens were collected from Turkey.

REFERENCES

Ačanski J, **Vujić A**, **Djan M**, **Obreht-Vidaković D**, **Ståhls G**, **Radenković S. 2016.** Defining species boundaries in the *Merodon avidus* complex (Diptera, Syrphidae) using integrative taxonomy, with the description of a new species. *European Journal of Taxonomy* **237:** 1–25.

Ačanski J, **Miličić M**, **Likov L**, **Milić D**, **Radenković S**, **Vujić A. 2017.** Environmental niche divergence of species from *Merodon ruficornis* group (Diptera: Syrphidae). *Archives of Biological Sciences* **69:** 247–259.

Andrić A, **Šikoparija B**, **Obreht D**, **Đan M**, **Preradović J**, **Radenković S**, **Pérez-Banon C**, **Vujić A. 2014.** DNA barcoding applied: identification of the larva of *Merodon avidus* (Diptera: Syrphidae). *Acta Entomologica Musei Nationalis Pragae* **54:** 741–757.

Arnqvist G, **Martensson T. 1998.** Measurement error in geo-metric morphometrics: empirical strategies to assess and reduce its impact on measures of shape. *Acta Zoologica Academiae Scientiarum Hungaricae* **44:** 73–96.

Bandelt HJ, **Forster P**, **Röhl A. 1999.** Median-joining networks for inferring intraspecific phylogenies. *Molecular Biology and Evolution* **16:** 37–48.

Barton N, **Jones JS. 1983.** Evolutionary biology: mitochondrial DNA: new clues about evolution. *Nature* **306:** 317–318.

Baylac M, **Frieß M. 2005.** Fourier descriptors, Procrustes superimposition, and data dimensionality: an example of cranial shape analysis in modern human populations. In: Slice DE, ed. *Modern morphometrics in physical anthropology*. Boston: Springer, 145–165.

Belshaw R, **Lopez-Vaamonde C**, **Degerli N**, **Quicke DL. 2001.** Paraphyletic taxa and taxonomic chaining: valuating the classification of braconine wasps (Hymenoptera: Braconidae) using 28S D2-3 rDNA sequences and morphological characters. *Biological Journal of the Linnean Society* **73:** 411–424.

Berggren WA. 1972. Late Pliocene–Pleistocene glaciation. In: Davies TA, ed. *Initial reports of the deep-sea drilling project*, **Vol. 12**. Washington, DC: US Government Printing Office, 953–963.

Borer M, **Alvarez N**, **Buerki S**, **Margraf N**, **Rahier M**, **Naisbit RE. 2010.** The phylogeography of an alpine leaf beetle: divergence within *Oreina elongata* spans several ice ages. *Molecular Phylogenetics and Evolution* **57:** 703–709.

Brown JL. 2014. SDMtoolbox: a python-based GIS toolkit for landscape genetic, biogeographic and species distribution model analyses. *Methods in Ecology and Evolution* **5:** 694–700.

Chen H, **Rangasamy M**, **Tan SY**, **Wang H**, **Siegfried BD. 2010.** Evaluation of five methods for total DNA extraction from western corn rootworm beetles. *PLoS One* **5:** e11963.

Chroni A, **Grković A**, **Ačanski J**, **Vujić A**, **Radenković S**, **Veličković N**, **Djan M**, **Petanidou T. 2018.** Disentangling a cryptic species complex and defining new species within the *Eumerus minotaurus* group (Diptera: Syrphidae), based on integrative taxonomy and Aegean palaeogeography. *Contributions to Zoology* **87:** 197–225.

Cowling DE, **Burnet B. 1981.** Courtship songs and genetic control of their acoustic characteristics in sibling species of the *Drosophila melanogaster* subgroup. *Animal Behaviour* **29:** 924–935.

Czerny L, **Strobl G. 1909.** Spanische Dipteren, III. *Beitrag Verh zool-bot Ges Wien* **59:** 121–301.

Dvořák L, **Ghahari H. 2016.** Distribution of *Panorpa nigrirostris* McLachlan, 1882, the single species of Mecoptera in Iran. *Acta Musei Moraviae, Scientiae Biologicae (Brno)* **101:** 1–5.

Fabricius JC. 1794. *Entomologia systematica emendata et aucta*, **Vol. 4**. Copenhagen: C. G. Proft, [6] + 472 + [5].

Fabricius JC. 1805. *Systema Antliatorum, secundum ordines, genera, species: adjectis synonymis, locis, observationibus, descriptionibus*. Braunschweig: C. Reichard, xiv + 15–372 +[1 (Errata)] + 30.

Funk DJ, **Omland KE. 2003.** Species-level paraphyly and polyphyly: frequency, causes, and consequences, with insights from animal mitochondrial DNA. *Annual Review of Ecology, Evolution, and Systematics* **34:** 397–423.

Folmer O, **Black M**, **Hoeh W**, **Lutz R**, **Vrijenhoek R. 1994.** DNA primers for amplification of mitochondrial cytochrome c oxidase subunit I from diverse metazoan invertebrates. *Molecular Marine Biology and Biotechnology* **3:** 294–299.

Goloboff PA. 1999. *NONA. – computer program, v.2.0*. Tucuman, Argentina: published by the author.

Hall TA. 1999. BioEdit: a user-friendly biological sequence alignment editor and analysis program for windows 95/98/NT. *Nucleic Acids Symposium Series* **41:** 95–98.

Harrison RG. 1989. Animal mitochondrial DNA as a genetic marker in population and evolutionary biology. *Trends in Ecology & Evolution* **4:** 6–11.

Harrison RG, **Larson EL. 2014.** Hybridization, introgression, and the nature of species boundaries. *Journal of Heredity* **105:** 795–809.

Hewitt GM. 2011. Mediterranean peninsulas: the evolution of hotspots. In: Zachos F, Habel J, eds. *Biodiversity hotspots*. Berlin, Heidelberg: Springer, 123–147.

Hijmans RJ, **Cameron SE**, **Parra JL**, **Jones PG**, **Jarvis A. 2005.** Very high resolution interpolated climate surfaces for global land areas. *International Journal of Climatology* **25:** 1965–1978.

Ivy-Ochs S, **Kerschner H**, **Reuther A**, **Preusser F**, **Heine K**, **Maisch M**, **Kubik PW**, **Schlüchter C. 2008.** Chronology of the last glacial cycle in the European Alps. *Journal of Quaternary Science* **23:** 559–573.

Jaskuła R, **Rewicz T**, **Płóciennik M**, **Grabowski M. 2016.** Pleistocene phylogeography and cryptic diversity of a tiger beetle, *Calomera littoralis*, in north-eastern Mediterranean and Pontic regions inferred from mitochondrial *COI* gene sequences. *PeerJ* **4:** e2128.

Katoh K, **Standley DM. 2013.** MAFFT multiple sequence alignment software, v.7: improvements in performance and usability. *Molecular Biology and Evolution* **30:** 772–780.

Available at: https://mafft.cbrc.jp/alignment/server/ (accessed 20 October 2019). doi: 10.1093/molbev/mst010.

Klingenberg CP. 2011. MORPHOJ: an integrated software package for geometric morphometrics, v.2.0. *Molecular Ecology Resources* **11:** 353–357.

Kočiš Tubić N, **Ståhls G**, **Ačanski J**, **Djan M**, **Obreht Vidaković D**, **Hayat R**, **Khaghaninia S**, **Vujić A**, **Radenković S. 2018.** An integrative approach in the assessment of species delimitation and structure of the *Merodon nanus* species group (Diptera: Syrphidae). *Organisms Diversity & Evolution* **18:** 479–497.

Kumar S, **Stecher G**, **Tamura K. 2016.** MEGA7: molecular evolutionary genetics analysis version 7.0 for bigger datasets. *Molecular Biology and Evolution* **33:** 1870–1874.

Lecocq T, **Dellicour S**, **Michez D**, **Lhomme P**, **Vanderplanck M**, **Valterová I**, **Rasplus JY**, **Rasmont P. 2013.** Scent of a break-up: phylogeography and reproductive trait divergences in the red-tailed bumblebee (*Bombus lapidarius*). *BMC Evolutionary Biology* **13:** 263.

Lipshutz SE. 2018. Interspecific competition, hybridization, and reproductive isolation in secondary contact: missing perspectives on males and females. *Current Zoology* **64:** 75–88.

Loew H. 1848. Ueber die europäischen Arten der Gattung *Eumerus*. *Stettiner Entomologische Zeitung* **9:** 108–128 + 130–136.

Loew H. 1862. Sechs neue europäische Dipteren. *Wiener Entomologische Monatsschrift* **6:** 294–300.

Macquart PJM. 1849. Huitième ordre. Les diptères, pp. 414–503. In: Lucas H, ed. *Exploration scientifique de l'Algérie pendant les années 1840, 1841, 1842 publiée par ordre du gouvernement et avec le concours d'une Commission Académique. Zoologie. Sciences Physiques. Histoire naturelle des animaux articulés. Troisième partie. Insectes*. Paris: Arthus Bertrand, 527.

Marcos-García MÁ, **Vujić A**, **Mengual X. 2007.** Revision of Iberian species of the genus *Merodon* (Diptera: Syrphidae). *European Journal of Entomology* **104:** 531–572.

Marcos-García MÁ, **Vujić A**, **Ricarte A**, **Ståhls G. 2011.** Towards an integrated taxonomy of the *Merodon equestris* species complex (Diptera: Syrphidae) including description of a new species, with additional data on Iberian *Merodon*. *The Canadian Entomologist* **143:** 332–348.

Martinet B, **Lecocq T**, **Brasero N**, **Biella P**, **Urbanova K**, **Valterova I**, **Cornalba M**, **Gjershaug JO**, **Michez D**, **Rasmont P. 2018.** Following the cold: geographical differentiation between interglacial refugia and speciation in the arcto-alpine species complex *Bombus monticola* (Hymenoptera: Apidae). *Systematic Entomology* **43:** 200–217.

Meigen JW. 1803. Versuch einer neuen Gattungs-Eintheilung der europaischen zweiflugligen Insekten. *Magazin für Insektenkunde* **2:** 259–281.

Meigen JW. 1822. *Systematische Beschreibung der bekannten europaischen zweiflugeligen Insekten. Vol. 3*. Hamm: Dritter Theil. Schulz-Wundermann, 416.

Mengual X, **Ståhls G**, **Vujić A**, **Marcos-García M. 2006.** Integrative taxonomy of Iberian *Merodon* species (Diptera: Syrphidae). *Zootaxa* **1377:** 1–26.

Menezes BF, **Vigoder FM**, **Peixoto AA**, **Varaldi J**, **Bitner-Mathé BC. 2013.** The influence of male wing shape on mating success in *Drosophila melanogaster*. *Animal Behaviour* **85:** 1217–1223.

Milankov V, **Ståhls G**, **Vujić A. 2008.** Genetic diversity of populations of *Merodon aureus* and *M. cinereus* species complexes (Diptera, Syrphidae): integrative taxonomy and implications for conservation priorities on the Balkan Peninsula. *Conservation Genetics* **9:** 1125–1137.

Miller MA, **Pfeiffer W**, **Schwartz T. 2010.** Creating the CIPRES Science Gateway for inference of large phylogenetic trees. *2010 Gateway Computing Environments Workshop (GCE)* New Orleans, LA, 1–8.

Monaghan MT, **Balke M**, **Gregory TR**, **Vogler AP. 2005.** DNA-based species delineation in tropical beetles using mitochondrial and nuclear markers. *Philosophical Transactions of the Royal Society B: Biological Sciences* **360:** 1925–1933.

Montgomery DC, **Peck EA. 1992.** *Introduction to linear regression analysis*, *2nd edn*. New York: Wiley-Interscience.

Naimi B. 2015. Usdm: uncertainty analysis for species. Distribution models. R package v.1.1–15. Available at: http://CRAN.R-project.org/package=usdm (accessed 12 April 2019).

Nedeljković Z, **Ačanski J**, **Vujić A**, **Obreht D**, **Đan M**, **Ståhls G**, **Radenković S. 2013.** Taxonomy of *Chrysotoxum festivum* Linnaeus, 1758 (Diptera: Syrphidae) – an integrative approach. *Zoological Journal of the Linnean Society* **169:** 84–102.

Nedeljković Z, **Ačanski J**, **Đan M**, **Obreht-Vidaković D**, **Ricarte A**, **Vujić A. 2015.** An integrated approach to delimiting species borders in the genus *Chrysotoxum* Meigen, 1803 (Diptera: Syrphidae), with description of two new species. *Contributions to Zoology* **84:** 285–304.

Nixon KC. 2008. ASADO, v..85 TNT-MrBayes Slaver v.2; mxram 200 (v.l 5.30). Made available through the author (previously named WinClada, version 1.00.08 (2002). Available at: http://www.diversityoflife.org/winclada (accessed 24 April 2018).

Outomuro D, **Adams DC**, **Johansson F. 2013.** The evolution of wing shape in ornamented winged damselflies (Calopterygidae, Odonata). *Evolutionary Biology* **40:** 300–309.

Parks DH, **Mankowski T**, **Zangooei S**, **Porter MS**, **Armanini DG**, **Baird DJ**, **Langille MGI**, **Beiko RG. 2013.** GenGIS 2: Geospatial analysis of traditional and genetic biodiversity, with new gradient algorithms and an extensible plugin framework. *PLoS One* **8:** e69885.

Phillips SJ, **Dudík M. 2008.** Modeling of species distributions with Maxent: new extensions and a comprehensive evaluation. *Ecography* **31:** 161–175.

Pinto-Juma GA, **Quartau JA**, **Bruford MW. 2008.** Population structure of *Cicada barbara* Stål (Hemiptera, Cicadoidea) from the Iberian Peninsula and Morocco based on mitochondrial DNA analysis. *Bulletin of Entomological Research* **98:** 15–25.

Popović D, **Ačanski J**, **Đan M**, **Obreht D**, **Vujić A**, **Radenković S. 2015.** Sibling species delimitation and nomenclature of the *Merodon avidus* complex (Diptera:

Syrphidae). *European Journal of Entomology* **112:** 790–809.

Preradović J, **Andrić A**, **Radenković S**, **Šašić Zorić L**, **Pérez-Bañón C**, **Campoy A**, **Vujić A. 2018.** Pupal stages of three species of the phytophagous genus *Merodon* Meigen (Diptera: Syrphidae). *Zootaxa* **4420:** 229–242.

R Development Core Team. **2016.** *R: a language and environment for statistical computing*. Vienna: R Foundation for Statistical Computing.

Radenković S, **Vujić A**, **Ståhls G**, **Pérez-Bañón C**, **Rojo S**, **Petanidou T**, **Šimić S. 2011.** Three new cryptic species of the genus *Merodon* Meigen (Diptera: Syrphidae) from the island of Lesvos (Greece). *Zootaxa* **2735:** 35–56.

Radenković S, **Veličković N**, **Ssymank A**, **Obreht Vidaković D**, **Djan M**, **Ståhls G**, **Veselić S**, **Vujić A. 2018a.** Close relatives of Mediterranean endemo-relict hoverflies (Diptera, Syrphidae) in South Africa: morphological and molecular evidence in the *Merodon melanocerus* subgroup. *PLoS One* **13:** e0200805.

Radenković S, **Šašić Zorić L**, **Djan M**, **Obreht Vidaković D**, **Ačanski J**, **Ståhls G**, **Veličković N**, **Markov Z**, **Petanidou T**, **Kočiš Tubić N**, **Vujić A. 2018b.** Cryptic speciation in the *Merodon luteomaculatus* complex (Diptera: Syrphidae) from the eastern Mediterranean. *Journal of Zoological Systematics and Evolutionary Research* **56:** 170–191.

Ricarte A, **Marcos-García MÁ**, **Rotheray GE. 2008.** The early stages and life histories of three *Eumerus* and two *Merodon* species (Diptera: Syrphidae) from the Mediterranean region. *Entomologica Fennica* **19:** 129–141.

Ritchie MG, **Gleason JM. 1995.** Rapid evolution of courtship song pattern in *Drosophila willistoni* sibling species. *Journal of Evolutionary Biology* **8:** 463–479.

Rodrigues AS, **Silva SE**, **Marabuto E**, **Silva DN**, **Wilson MR**, **Thompson V**, **Yurtsever S**, **Halkka A**, **Borges PAV**, **Quartau JA**, **Paulo OS**, **Seabra SG. 2014.** New mitochondrial and nuclear evidences support recent demographic expansion and an atypical phylogeographic pattern in the spittlebug *Philaenus spumarius* (Hemiptera, Aphrophoridae). *PLoS One* **9:** e98375.

Rodríguez F, **Oliver JL**, **Marín A**, **Medina JR. 1990.** The general stochastic model of nucleotide substitution. *Journal of Theoretical Biology* **142:** 485–501.

Rohlf FJ. 2006. *TpsDig – digitize landmarks and outlines, v.2.05*. Stony Brook: Department of Ecology and Evolution, State University of New York.

Rohlf FJ, **Slice DE. 1990.** Extensions of the Procrustes method for the optimal superimposition of landmarks. *Systematic Biology* **39:** 40–59.

Routtu J, **Mazzi D**, **Van Der Linde K**, **Mirol P**, **Butlin RK**, **Hoikkala A. 2007.** The extent of variation in male song, wing and genital characters among allopatric *Drosophila montana* populations. *Journal of Evolutionary Biology* **20:** 1591–1601.

Rutschmann F. 2006. Molecular dating of phylogenetic trees: a brief review of current methods that estimate divergence times. *Diversity and Distributions* **12:** 35–48.

Sacchi R, **Hardersen S. 2013.** Wing length allometry in Odonata: differences between families in relation to migratory behaviour. *Zoomorphology* **132:** 23–32.

Šašić L, **Ačanski J**, **Vujić A**, **Ståhls G**, **Radenković S**, **Milić D**, **Obreht Vidaković D**, **Đan M. 2016.** Molecular and morphological inference of three cryptic species within the *Merodon aureus* species group (Diptera: Syrphidae). *PLoS One* **11:** e0160001.

Šašić Zorić L, **Ačanski J**, **Đan M**, **Kočiš Tubić N**, **Veličković N**, **Radenković S**, **Vujić A. 2018.** Integrative taxonomy of *Merodon caerulescens* complex (Diptera: Syrphidae) – evidence of cryptic speciation. *Matica Srpska Journal for Natural Sciences* **135:** 103–118.

Sánchez-Guillén RA, **Córdoba-Aguilar A**, **Hansson B**, **Ott J**, **Wellenreuther M. 2016.** Evolutionary consequences of climate-induced range shifts in insects. *Biological Reviews* **91:** 1050–1064.

Schmid U. 1999. Schwebfliegen-Nachweise (Diptera, Syrphidae) aus Deutschland: *Cheilosia laeviseta* Claussen, 1987, *Merodon aeneus* Meigen, 1822 und *Syrphus auberti* Goeldlin de Tiefenau, 1996. *Volucella* **4:** 161–165.

Schmitt T. 2007. Molecular biogeography of Europe: Pleistocene cycles and postglacial trends. *Frontiers in Zoology* **4:** 11.

Schmitt T, **Muster C**, **Schönswetter P. 2010.** Are disjunct Alpine and Arctic-Alpine animal and plant species in the western Palearctic really 'relics of a cold past'. In: Habel JC, Assmann T, eds. *Relict species*. Berlin, Heidelberg: Springer, 239–252. doi: 10.1007/978-3-540-92160-8_13.

Schmitt T, **Louy D**, **Zimmermann E**, **Habel JC. 2016.** Species radiation in the Alps: multiple range shifts caused diversification in ringlet butterflies in the European high mountains. *Organisms Diversity & Evolution* **16:** 791–808.

Schneider T, **Ikemeyer D**, **Mueller O**, **Dumont HJ. 2018.** Checklist of the dragonflies (Odonata) of Iran with new records and notes on distribution and taxonomy. *Zootaxa* **4394:** 1–40.

Schoener TW. 1968. The anolis lizards of Bimini: resource partitioning in a complex fauna. *Ecology* **49:** 704–726.

Šimić S, **Vujić A. 1997.** Hoverfly fauna (Diptera: Syrphidae) of the southern part of the mountain Stara Planina, Serbia. *Acta Entomologica Serbica* **2:** 21–30.

Simon C, **Frati F**, **Beckenbach A**, **Crespi B**, **Liu H**, **Flook P. 1994.** Evolution, weighting, and phylogenetic utility of mitochondrial gene sequences and a compilation of conserved polymerase chain reaction primers. *Annals of the Entomological Society of America* **87:** 651–701.

Soltis PS, **Soltis DE. 2003.** Applying the bootstrap in phylogeny reconstruction. *Statistical Science* **18:** 256–267.

Speight MCD. 2018. Species accounts of European Syrphidae, 2018. In: Speight MCD, Castella E, Sarthou J-P, Vanappelghem C, eds. *Syrph the net, the database of European Syrphidae (Diptera)*, **Vol. 103**. Dublin: Syrph the Net publications, 302.

Ståhls G, **Vujić A**, **Pérez-Bañón C**, **Radenković S**, **Rojo S**, **Petanidou T. 2009.** *COI* barcodes for identification of *Merodon* hoverflies (Diptera, Syrphidae) of Lesvos Island, Greece. *Molecular Ecology Resources* **9:** 1431–1438.

Stamatakis A. 2014. RAxML version 8: a tool for phylogenetic analysis and post-analysis of large phylogenies. *Bioinformatics* **30:** 1312–1313.

Statistica D. 2015. *Dell Statistica data analysis software system, v.13*. Round Rock, TX: Dell Inc.

Stubbs AE, **Falk S. 1983.** *British hoverflies: an illustrated guide*. London: British Entomological and Natural History Society.

Tauber E, **Eberl DF. 2003.** Acoustic communication in *Drosophila*. *Behavioural Processes* **64:** 197–210.

Thompson FC. 1999. Key to the genera of the flower flies (Diptera: Syrphidae) of the Neotropical Region including descriptions of new genera and species and a glossary of taxonomic terms. *Contributions on Entomology, International* **3:** 321–378.

Thompson FC, **Brake I. 2005.** *Biosystematic database of world Diptera*. Systema Dipterorum. Available at: https://web.archive.org/web/20180615024537/http://www.diptera.org/ (accessed 8 November 2018).

Van de Weyer G, **Dils J. 1999.** Contribution to the knowledge of the Syrphidae from Greece (Diptera: Syrphidae). *Phegea* **27:** 69–77.

Veselić S, **Vujić A**, **Radenković S. 2017.** Three new eastern-Mediterranean endemic species of the *Merodon aureus* group (Diptera: Syrphidae). *Zootaxa* **4254:** 401–434.

Vujić A, **Šimić S**, **Radenković S. 1995.** *Merodon desuturinus*, a new hoverfly (Diptera: Syrphidae) from the mountain Kopaonik (Serbia). *Ekologija* **30:** 65–70.

Vujić A, **Radenković S**, **Ståhls G**, **Ačanski J**, **Stefanović A**, **Veselić S**, **Andrić A**, **Hayat R. 2012.** Systematics and taxonomy of the *ruficornis* group of genus *Merodon* Meigen (Diptera: Syrphidae). *Systematic Entomology* **37:** 578–602.

Vujić A, **Radenković S**, **Likov L**, **Trifunov S**, **Nikolić T. 2013a.** Three new species of the *Merodon nigritarsis* group (Diptera: Syrphidae) from the Middle East. *Zootaxa* **3640:** 442–464.

Vujić A, **Ståhls G**, **Ačanski J**, **Bartsch H**, **Bygebjerg R**, **Stefanović A. 2013b.** Systematics of Pipizini and taxonomy of European *Pipiza* Fallén: molecular and morphological evidence (Diptera, Syrphidae). *Zoologica Scripta* **42:** 288–305.

Vujić A, **Radenković S**, **Ačanski J**, **Grković A**, **Taylor M**, **Şenol SG**, **Hayat R. 2015.** Revision of the species of the *Merodon nanus* group (Diptera: Syrphidae) including three new species. *Zootaxa* **4006:** 439–462.

Vujić A, **Ståhls G**, **Ačanski J**, **Rojo S**, **Pérez-Bañón C**, **Radenković S. 2018.** Review of the *Merodon albifasciatus* Macquart species complex (Diptera Syrphidae): the nomenclatural type located and its provenance discussed. *Zootaxa* **4374:** 25–48.

Wang Y, **Zhou QS**, **Qiao HJ**, **Zhang AB**, **Yu F**, **Wang XB**, **Zhu CD**, **Zhang YZ. 2016.** Formal nomenclature and description of cryptic species of the *Encyrtus sasakii* complex (Hymenoptera: Encyrtidae). *Scientific Reports* **6:** 34372.

Warren DL, **Glor RE**, **Turelli M. 2008.** Environmental niche equivalency versus conservatism: quantitative approaches to niche evolution. *Evolution: International Journal of Organic Evolution* **62:** 2868–2883.

Warren DL, **Glor RE**, **Turelli M. 2010.** ENMTools: a toolbox for comparative studies of environmental niche models. *Ecography* **33:** 607–611.

Zelditch ML, **Swiderski DL**, **Sheets HD**, **Fink WL. 2004.** *Geometric morphometrics for biologists: a primer*. London: Elsevier Academic Press.

Zhou X, **Kjer KM**, **Morse JC. 2007.** Associating larvae and adults of Chinese Hydropsychidae caddisflies (Insecta: Trichoptera) using DNA sequences. *Journal of the North American Benthological Society* **26:** 719–742.

Zimsen E. 1964. *The type material of I.C. Fabricius*. Copenhagen: Munksgaard, 508.

SUPPORTING INFORMATION

Additional Supporting Information may be found in the online version of this article at the publisher's web-site.

File S1. 28S rRNA gene sequence alignment.
File S2. Combined 5' and 3'*COI* gene sequence alignment.
Table S1. List of specimens of *Merodon aureus* subgroup used for molecular and geometric morphometric analyses.
Table S2. List of 28S rRNA gene genotypes of *Merodon aureus* subgroup.
Appendix S1. Other material analysed.
Figure S1. The *COI* gene strict consensus tree of the *Merodon aureus* subgroup. Filled circles ●stand for unique changes, open circles ○ stand for non-unique; bootstrap values ≥ 50 are presented near nodes.